Bio-Design and Manufacturing (2023) 6:51–73
https://doi.org/10.1007/s42242-022-00212-4

REVIEW

Novel structural designs of 3D-printed osteogenic graft for rapid angiogenesis

Weiying Lu[1,2,3,4] · **Yang Shi**[1,2,3,4] · **Zhijian Xie**[1,2,3,4]

Received: 9 May 2022 / Accepted: 8 September 2022 / Published online: 13 October 2022
© Zhejiang University Press 2022

Abstract

Large bone defect regeneration has always been recognized as a challenging clinical problem due to the difficulty of revascularization. Conventional treatments exhibit certain inherent disadvantages (e.g., secondary injury, immunization, and potential infections). However, three-dimensional (3D) printing technology as an emerging field can serve as an effective approach to achieve satisfactory revascularization while making up for the above limitations. A wide variety of methods can be used to facilitate blood supply during the design of a 3D-printed scaffold. Importantly, the scaffold structure lays a foundation for the entire printing object; any method to promote angiogenesis can be effective only if it is based on well-designed scaffolds. In this review, different designs related to angiogenesis are summarized by collecting the literature from recent years. The 3D-printed scaffolds are classified into four major categories and discussed in detail, from elementary porous scaffolds to the most advanced bone-like scaffolds. Finally, structural design suggestions to achieve rapid angiogenesis are proposed by analyzing the above architectures. This review can provide a reference for organizations or individual academics to achieve improved bone defect repair and regeneration using 3D printing.

Graphic abstract

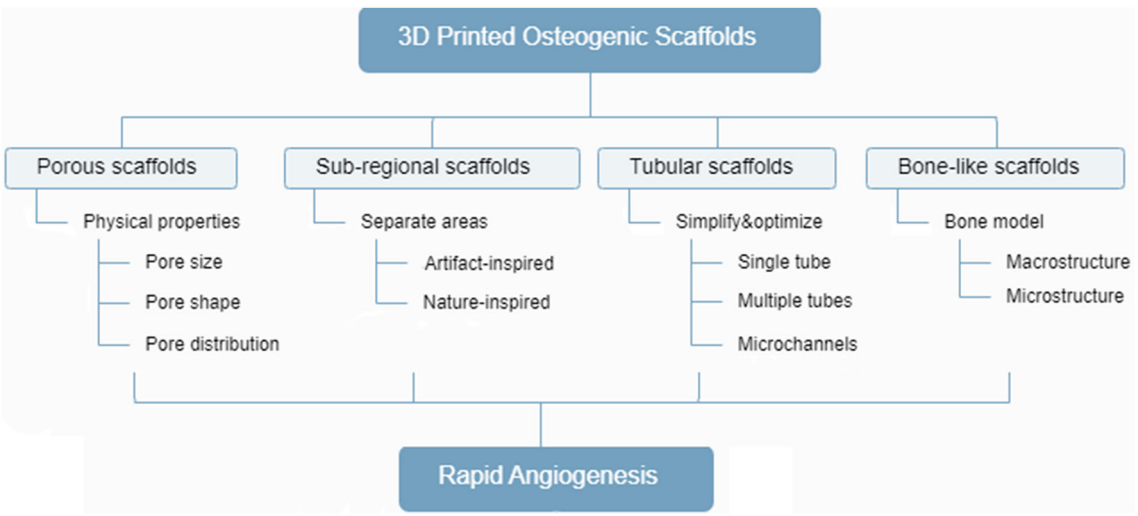

Keywords 3D printing · Angiogenesis · Bone regeneration · Tissue engineering · Biomimetic scaffolds

✉ Zhijian Xie
xzj66@zju.edu.cn

[1] Stomatology Hospital, School of Stomatology, Zhejiang University School of Medicine, Zhejiang University, Hangzhou 310006, China

[2] Key Laboratory of Oral Biomedical Research of Zhejiang Province, Zhejiang University, Hangzhou 310006, China

[3] Cancer Center, Zhejiang University, Hangzhou 310006, China

[4] Zhejiang Provincial Clinical Research Center for Oral Diseases, Zhejiang University, Hangzhou 310006, China

Introduction

Bone defects imply damage to the integrity of the bone structure [1]. Such defects should be treated by surgical intervention, especially when the size of the defect exceeds the limit of the body's self-repair ability [2, 3]. The major aim is to avoid physical or psychological harm to patients [4, 5]. Autografts have been considered as the clinical gold standard for healing the above bone defects, which are capable of preserving natural blood vessels and nerve fibers around the donor tissue [6]. Thus, the bone graft can be integrated into the recipient area and achieve repair in a relatively short period [7]. Autologous transplantation, however, has shown numerous disadvantages, e.g., secondary injuries, limited donor tissue, and sequelae of donor site removal [8–10]. Meanwhile, synthetic materials have become increasingly common in clinical practice over the past few years [11]. Traditional grafts are dominated by non-degradable metals and ceramic scaffolds [12]. They are sufficiently dense and strong to replace bone in the body for extended periods; however, these materials and casting methods lack osteoconductivity, hence they fail to achieve well-organized regeneration in defective areas. Besides, inadequate self-tissue and blood supply can cause complications (e.g., infection and ischemic necrosis) after transplantation.

Bone, a type of highly vascularized tissue, cannot complete its regeneration process without blood supply [13–15]. The repair of the fracture is initiated by blood vessels, blood cells, and relevant substances (Fig. 1) [16]. Moreover, the blood supply at the site of a bone defect has a direct effect on the healing status. For instance, the vascular distribution of the femoral neck causes femoral neck fractures to be highly susceptible to ischemic necrosis of the femoral head, and tibial stem fractures with less surface soft tissue coverage are prone to delayed healing. It is well known that cells are dependent on capillaries for survival in the human body. Oxygen and nutrients in capillaries can only diffuse as far as 200 μm under physiological conditions [6, 17–19]. Thus, capillaries are widely distributed to ensure the normal functioning of all cells. As a result, the lack of blood supply and circulation to the graft will lead to its failure of integration, internal graft necrosis, among other problems, causing exacerbated harm to the host [20–22]. The internal blood supply of large implants required for large bone defects is commonly difficult or impossible to establish in a timely manner using conventional materials and techniques [23–25].

Grafts made by three-dimensional (3D) printing technology are currently expected to replace traditional grafts [26]. The 3D-printed scaffolds, formed by different raw materials and fine structures, are capable of minimizing complications arising from insufficient blood supply [27, 28]. Furthermore, grafts are endowed with an individualized and specific shape, which can be more extensively employed in bone defects all over the body [2, 29]. As revealed by the above analysis, rapid vascularization has critical significance for grafts to achieve integration and osteogenesis [29–31]. Moreover, the rapidly developing 3D printing technique provides several ideal solutions for the angiogenesis problem, such as pre-vascularization, component modification, and design modification [1, 32]. The first two methods possess special advantages. The transplantation of a pre-vascularized scaffold with an autologous vascular bundle is more of a compromise for the autograft [33–35]. It does have the facility for quick perfusion; however, direct suturing between vascular bundles may cause several complications (e.g., thrombosis and stenosis) [36, 37]. In addition, there are pre-vascularization methods in which the scaffolds are first incubated on highly vascularized soft tissue to form a microvascular network before being grafted to the defect site [38, 39], although these methods are also burdened (e.g., secondary damage) [40, 41]. At the moment, scaffold angiogenesis is being investigated through component modification (e.g., altering the scaffold material and adding vital angiogenic factors) [42, 43]. The addition of growth factors, including vascular endothelial growth factor (VEGF), platelet-derived growth factor (PDGF), and fibroblast growth factor 2 (FGF2), has been the most extensively used technique [44–47]. While the above biomolecules show excellent angiogenic capabilities, they have some disadvantages, such as complex loading patterns, potential immune response, and difficult concentration control [48, 49]. The incorporation of exosomes into the scaffolds as a component modification is another direction at the forefront of related research [43, 50]. In comparison with directly added growth factors, exosomes work better and have fewer side effects [51]. Scaffolds with exosomes are still being investigated, in which exosomes are responsible for the main mechanism of action; therefore, such scaffolds are not discussed in much detail in this review.

It is common practice to use several of the above pre-angiogenic methods in combination, where the scaffold is the foundation of the entire 3D-printed bone graft, and other components form the superstructure. The effectiveness of any method in promoting vascularization can be maximized when the scaffold structure is carefully designed. Hence, this review provides cutting-edge results on 3D-printed bone tissue covering the past few years of literature while assessing the currently available scaffold structure designs to achieve rapid vascularization. The following is a summary of a range of structures from basic forms to complex bone-like constructs. The most basic porous scaffolds are described by certain parameters (e.g., aperture size, shape, and distribution). Furthermore, there are innovative scaffolds with sub-regional, tubular, and bone-like scaffolds. This review analyzes and summarizes the common scaffold structure

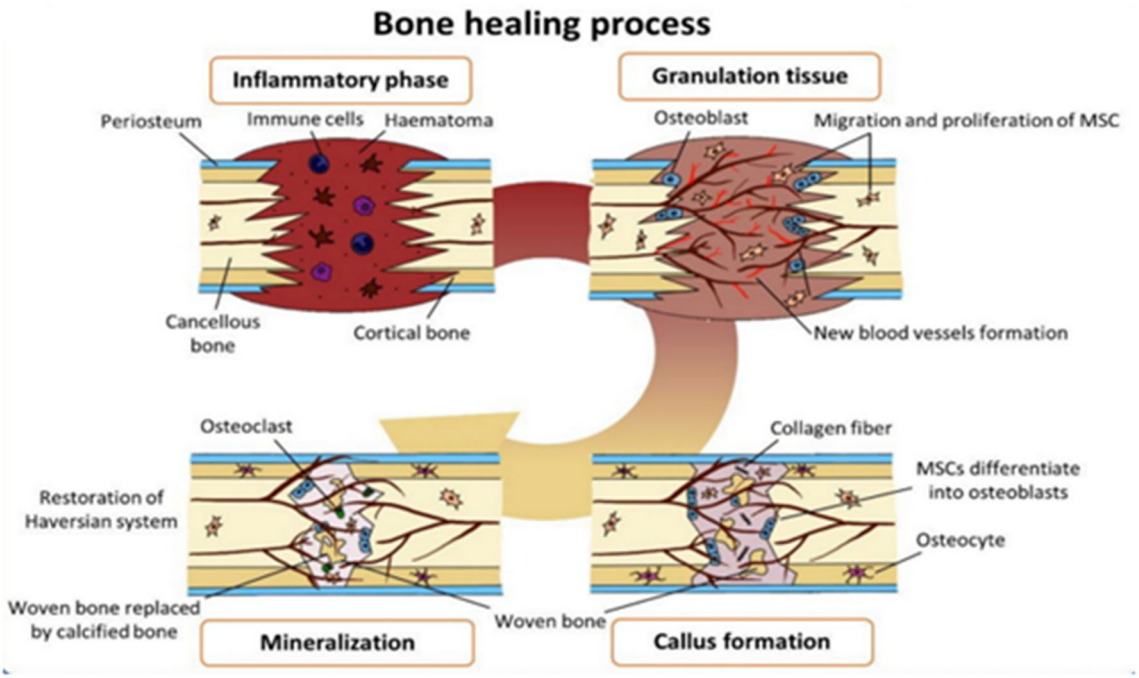

Fig. 1 Schematic diagram of femoral fracture repair period (reproduced from Park et al. [20], Copyright 2021, with permission from the authors)

designs that can facilitate angiogenesis, which can be conducive to the design of osteogenic grafts that have higher compatibility with the physiological characteristics of the human body in the future.

Porous scaffolds

In most of the existing studies on 3D-printed bone grafts, the scaffold design is the simplest mesh shape, which promotes highlighting the role of different materials of scaffolds or different added substances on osteogenesis and vascularization in experimental investigations. Even for the simplest structure, there are differences, and various parameters (e.g., porosity, pore size, shape, and connectivity between pores) are adjustable in the porous scaffold to facilitate blood vessel growth [52, 53].

Pore size

The internal and external structural morphology of grafts can be precisely controlled by 3D printing [54, 55]. Pores exhibiting similar structures are grouped together to form a porous scaffold, and the respective pores are interconnected with another type to create a complex internal space that promotes cell migration and growth, enhancing circulation integration and fluid exchange [56].

When the pore size is approximately 100 μm, the cells are capable of crawling into the pore and generating bone tissue [57]. However, this is insufficient to support vascular invasion. It has been generally accepted that the pore size should be at least greater than 300 μm to form a normal capillary structure [52, 58, 59]. Even though pre-vascular cells can grow in small-sized pores (100–200 μm), their inability to form a luminal structure capable of transporting oxygen and nutrients results in a relatively hypoxic environment within the pore [60]. This stimulates the formation of more matrix deposits by bone mesenchymal stem cells (BMSCs), such as glycosaminoglycan and collaged type II, while it facilitates the differentiation of BMSC to chondrocytes [61, 62]. In addition, the hypoxic environment and the small holes present will be conducive to the reproduction of bacteria, resulting in infections [63].

In contrast, the capillary branches of external blood vessels can penetrate and communicate with the interior of the graft due to their large size, thus playing a role in the blood circulation of the host, ensuring the smooth diffusion of nutrients and oxygen, and directly inducing cellular osteogenesis [64]. Moreover, the larger internal space encourages new capillaries to mature and blood vessels to form with complete function and structure [65]. It is therefore concluded that the larger the pore size, the better the blood vessel growth. Meanwhile, pore size has an upper limit for the promotion of angiogenesis. Also, cells recognize the surface of the fibrous scaffold as a planar substrate instead of a 3D porous structure, thereby the advantage of the scaffold is lost [66]. Accordingly, the recommended pore size setting should be between 500 and 1200 μm.

Pore shape

A larger pore size facilitates angiogenesis while decreasing the mechanical properties of the scaffold [67–69]. Therefore, the mechanical properties of an osteogenic scaffold should be maintained while pursuing large pore sizes to promote blood vessel growth. One of the suitable methods is to change the pore shape and stacking method. The various stacking methods for the shape change of the pores in the porous scaffold of the repeating unit structure are very similar.

Besides the conventional architecture, planar structures (e.g., triangles and hexagons) and stereo structures (e.g., octahedrons and topologies) are also employed in the scaffolds [70, 71]. The pore geometry is capable of influencing the growth and adhesion of cells [72]. A larger curvature can boost cells to grow faster; hence, porous scaffolds with sharp triangles are more conducive to tissue invasion and formation [73]. Nonetheless, with larger curvature, the pores become narrower and tissue infestation becomes harder (Fig. 2a) [74]. In comparison with other shapes, the hexagonal shape can transfer stresses more uniformly across the scaffold, similar to a circle (Fig. 2b) [75]. Thus, hexagons exhibit high fatigue resistance and compressive strength [76]. The above two properties play a vital role in grafts replacing bone tissue to perform their function [77]. Octahedron, as a stereo-structure, has stronger resistance to pressure (Fig. 2c) [78]. Moreover, the topological stereo-structure is found to significantly increase the biodegradation rate of the scaffold (Fig. 2d) [79, 80]. This finding may be correlated with the high level of interconnectivity, thus enhancing the permeability and the velocity [81, 82]. The circulation of body fluids in the scaffold is accelerated, which facilitates internal access to oxygen and nutrients and also stimulates vascular maturation [83]. Each pore shape has its own advantages, and this review is only a brief compilation of their main features; researchers should select the right shape in accordance with their needs.

Pore distribution

As discussed above regarding pore size, different sizes perform different functions. The gradient density scaffold takes advantage of this fact based on the different requirements for vessel growth, in which pores of different sizes are arranged in a regular pattern on the scaffold. Scaffolds with a top-to-bottom density gradient have been largely utilized in graft designs where cartilage and bone are regenerated simultaneously (Fig. 3a) [64, 84, 85]. The high-density upper layer forms a hypoxic environment promoting cellular cartilage differentiation, while the sparse lower layer generates normal bone tissue with blood vessels that provide support and nourishment [86]. The underlying vasculature has critical significance for the regeneration and repair of cartilage tissue [87].

Scaffolds showing a gradient density difference between the inside and the outside significantly contribute to tissue regeneration (Fig. 3b). It has been demonstrated by experiments that dense and lax exteriors are beneficial for scaffold-host integration [82]. In addition, gradient density scaffolds are more resilient [88]. In comparison with constant scaffolds, the dense interior facilitates faster inward invasion of the tissue instead of too early maturation at the periphery. Before considering vascular maturation, the infiltration of the vascular system for the scaffold should be ensured first to avoid central necrosis. Both the number of vessels and their maturity are vital factors in this regard [89]. A larger external pore size allows the base section of vessels to begin to mature first, ensuring the normal function of the vascular system and avoiding the possibility of blood vessels breaking and leaking at a later stage. Moreover, the density gradient leads to a flow rate gap in the scaffold. Faster external flow rates enable internal metabolic waste to leave more quickly and nutrients to enter more rapidly, which explains why gradient density scaffolds can inoculate cells more uniformly [90, 91].

In general, the porous structure achieves the purpose of promoting vascular regeneration through the stimulation of angiogenic endothelial cells through its physical properties in the microenvironment inside the scaffolds, including but not limited to the parameters mentioned above. Regarding the specific mechanisms, the reader is referred to the literature [92]. Although there are more changes in terms of pore shape and distribution, the pore size is the ultimate dominating factor [93, 94]. As the pore size increases, the porosity is enhanced, and the permeability and degradation efficiency can also be enhanced, thus contributing to the generation of blood vessels and bone tissue [93]. However, the mechanical properties and biological functions are in a conflicting relationship and need to be balanced [2, 62]. Different parts of the bone under different stresses perform various functions, and the mechanical properties necessary for grafts are significantly diverse. Accordingly, the ideal setting of these properties should be weighed on a case-by-case basis.

Other factors may also have an effect on the equilibrium point, including the nature of the scaffold material. The current commonly applied methods of 3D printing include stereolithography (SLA), fused deposition modeling (FDM), and selective laser sintering (SLS) [23, 31, 70]. In comparison with digital drawing designs, the printed object will have certain differences due to the actual steps during the printing process. The effect of the printing method on the product has been discussed in other reviews and will not be elucidated in this review [95, 96]. Lastly, the various factors added to the scaffold also have subtle effects on the morphological structure [97–99]. It is noteworthy that these fine changes are imperceptible to humans, whereas they can be quite significant for cells growing in it.

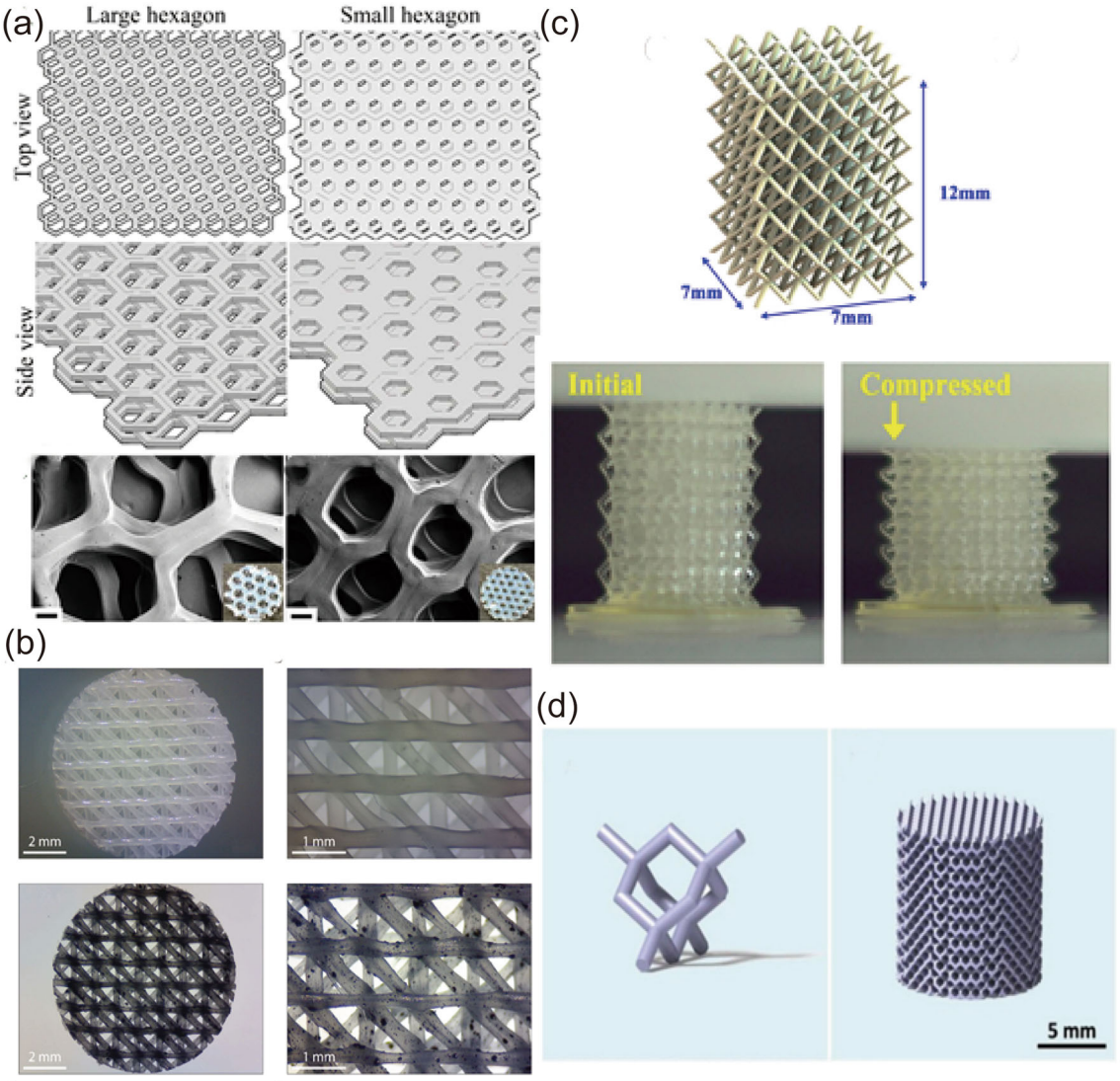

Fig. 2 **a** CAD models of scaffolds with large and small hexagonal shapes (reproduced from Zhou et al. [74], Copyright 2016, with permission from the authors). **b** Stereomicroscopic images of scaffolds with triangular pores (reproduced from Lopez-Gonzalez et al. [75], Copyright 2021, with permission from the authors). **c** 3D model of octahedron scaffold and the photograph of initial and compressed octahedron scaffold (reproduced from Xue et al. [78], Copyright 2019, with permission from American Chemical Society). **d** Topological unit and entire topological scaffold structure (reproduced from Li et al. [81], Copyright 2018, with permission from Elsevier)

Sub-regional scaffolds

The porous scaffold is relatively fixed in its general form, with an overall columnar shape and a repeating unit structure inside. It has been confirmed by numerous experiments that it is necessary to differentiate the osteogenic region from the vasculogenic region to facilitate the growth of blood vessels. The ink in the angiogenic region can be degraded earlier [100], loaded with important factors that induce blood vessel growth [101], or allow cells to grow directly in it [102]. The design difficulty and novelty of the above type of scaffold primarily concern the distribution and construction of the angiogenic part in the whole scaffold. Researchers have been inspired by diverse life forms to propose some innovative designs for the scaffolds; some examples are listed below.

Artifact-inspired structures

Layered distribution

In this type of sub-regional scaffold, different regions are printed in layers and then stacked. A layer of gel for blood vessel generation is added between two layers of the osteogenic scaffold, forming a sandwich-like scaffold

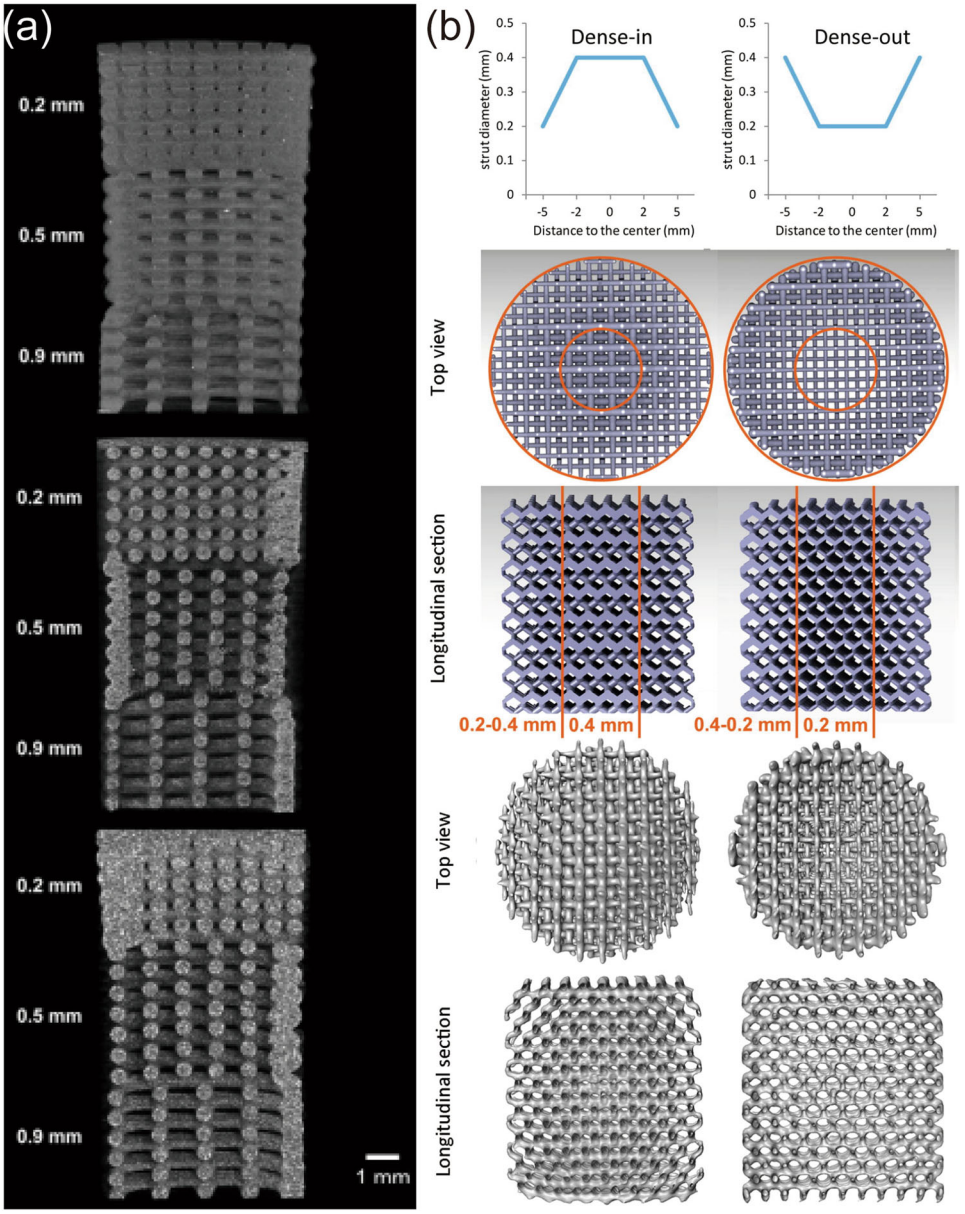

Fig. 3 **a** Scaffolds with a top-to-bottom density gradient. Scale bar = 1 mm (reproduced from Bittner et al. [84], Copyright 2019, with permission from Elsevier). **b** The designs of gradient density scaffolds including dense-in and dense-out: strut size distribution, top view and longitudinal cross section of the CAD models, and the micro-CT reconstructions of the AM porous iron specimens (reproduced from Li et al. [82], Copyright 2019, with permission from Elsevier)

[83]. This gel is composed of GelMA, a relatively soft material, into which vascular structures could invade easily. The center is sacrificed by polyvinyl alcohol (PVA) to form a Y-like pathway with a duct diameter of 800 μm (Fig. 4a). The channel is adopted to simulate large blood vessels in vivo. The perfusable vessel channel significantly facilitates the overall scaffold angiogenesis [103]. Notably, this scaffold is educated in a dynamic culture for in vitro experiments. Compared with the traditional static culture, the dynamic culture is superior in all indicators and more closely resembles the in vivo environment [104, 105].

If this structure is repeated many times, it forms a lasagna-like scaffold (Fig. 4b). Electrospun fiber membranes are alternately stacked with polycaprolactone (PCL) scaffolds to form a lasagna-like monolithic structure. Gelatin electrospun fibrous scaffolds can enhance the overall hydrophilicity of the scaffold and facilitate cell adhesion and proliferation [106]. Also, the physical properties of electrospun fiber membranes immunomodulate macrophages, inhibiting the M1 phenotype while activating the M2 phenotype [107, 108], which has been proved to significantly facilitate osteogenesis and angiogenesis [42, 109, 110]. Moreover, in vivo experiments have confirmed that scaffolds with lasagna-like structures exhibit more neovascularization. The physical properties of the scaffold also determine its mechanical features while controlling tissue regeneration and immune modulation [111, 112], which is one of the reasons that inspired this review; we also aimed to highlight the importance of the structural layout of the scaffold.

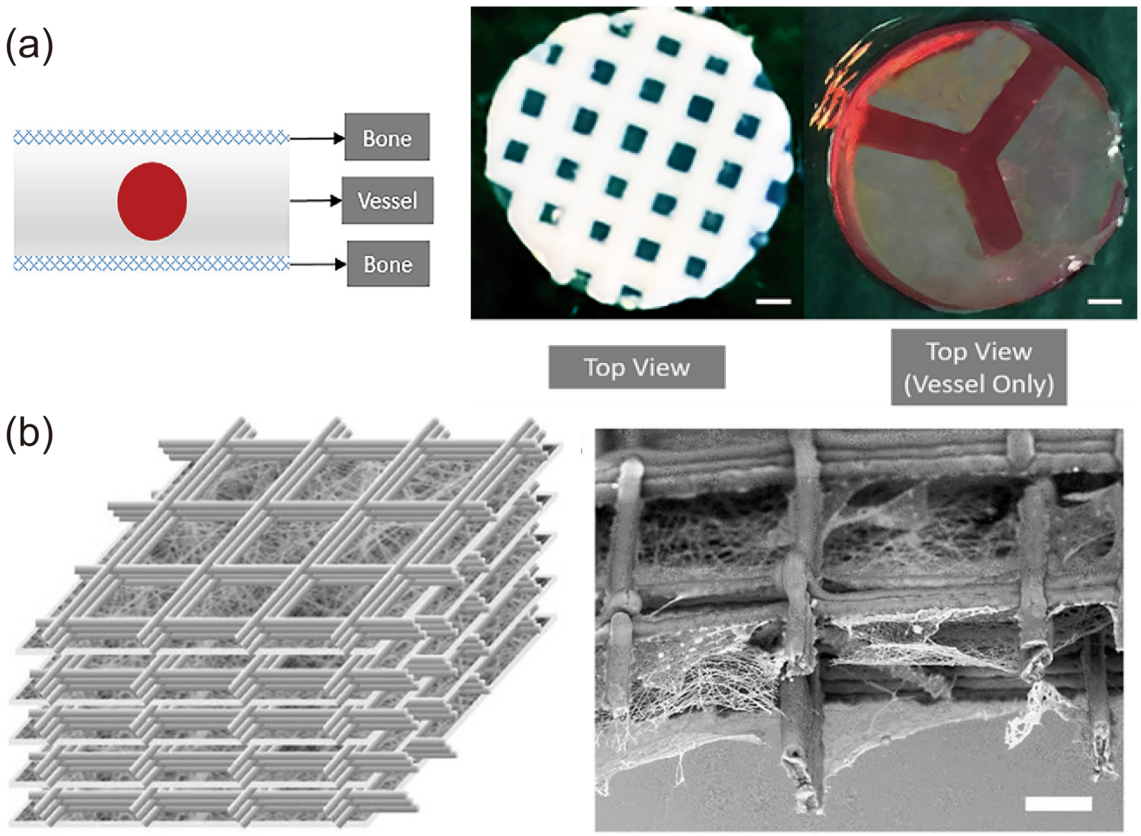

Fig. 4 **a** Concept of the sandwich-like scaffold. Photographs of the bone layer and vascular layer (top view). Scale bar = 1 mm (reproduced from Hann et al. [83], Copyright 2021, with permission from Elsevier). **b** Schematic illustration and SEM image of lasagna-like scaffolds. Scale bar = 40 μm (reproduced from Wang et al. [106], Copyright 2021, with permission from Elsevier)

Core–shell distribution

Unlike in layered distribution, the core–shell structure distinguishes two functional regions on the same fiber. For example, alginate shell-wrapped calcium-deficient hydroxyl apatite (CDHA) core is fabricated by coaxial printing to form a CD-like structure [113]. The two assume different functions while complementing each other: the core enhances the overall mechanical strength, and the hydrogel compensates for the brittle nature of the ceramic (Fig. 5a). Different from the usual scaffolds, this type has a shell from a soft cell-loaded hydrogel, which comes into full contact with the outside environment to ensure the physiological needs of the cells. In this scaffold, during the entire culture period (35 days), almost all cells preserve their viability. This is an important consideration as cellular activity should be ensured first, which is of critical significance in the loaded cell scaffold design.

Furthermore, coaxial printing can be combined with sacrificial ink. The sacrificial template technique has been increasingly applied in the construction of complex vascular systems [114]. Some low-toxicity sacrificial inks can even carry cells [115–117]. Endothelial cell-rich sacrificial ink is coaxially printed with outer scaffold ink (Fig. 5b). After the sacrificial ink has been removed, the endothelial cells cling to a tubular scaffold, which forms a vascular-like structure that takes its position before true angiogenesis [118, 119]. This kind of sacrificial ink solves the problem of uniformly seeding cells inside complex structures. The above type of structure is simultaneously adaptable to different needs (e.g., drug delivery) (Fig. 5c). The materials or factors of the inner or outer parts can be varied based on the design requirements [120, 121].

Nature-inspired structures

Olive-shaped structure (Fig. 6a): The scaffold is primarily formed by a monophasic calcium phosphate cement (CPC), with some CPC chains replaced by alginate–gellan gum (AlgGG) since the peripheral vessels of the graft are easier to invade [122]. The number of AlgGG substitution chains increases from the layer adjacent to the natural bone toward the center of the scaffold [123]. This structure shows an olive-shaped distribution with fewer ends and more material in the center. Moreover, the printing direction between the layers is

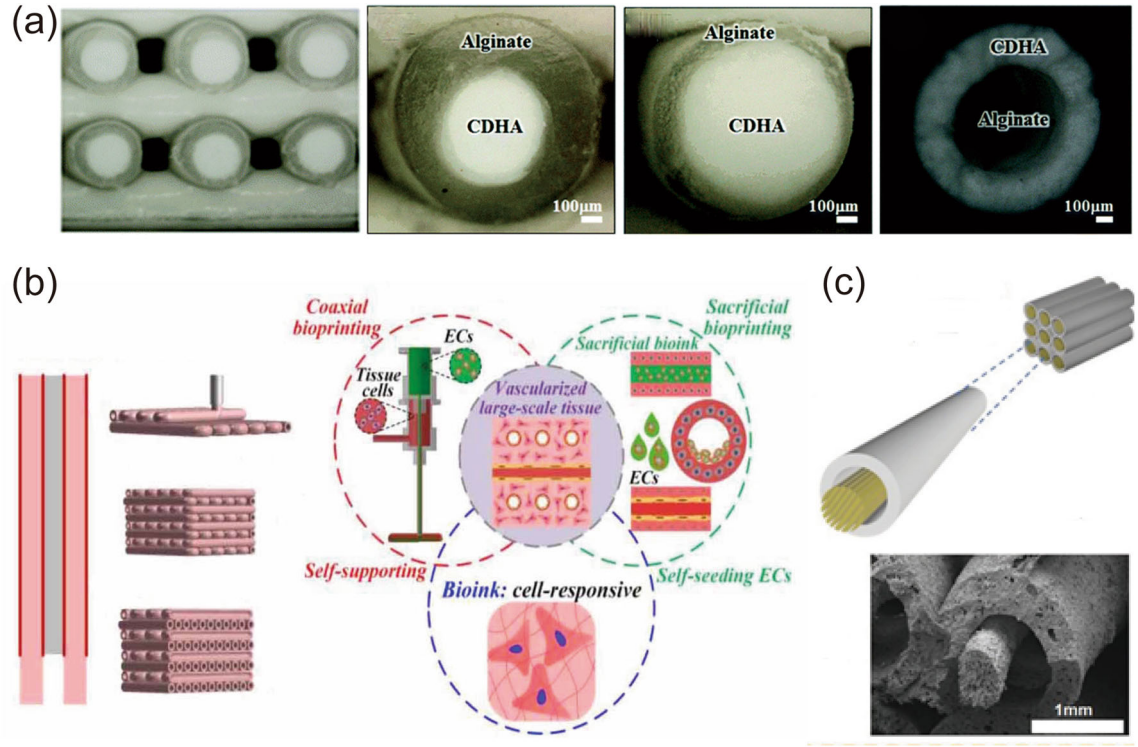

Fig. 5 **a** Optical images of CD-like scaffolds: the longitudinal view of the scaffold, the cross section of scaffold strut with different shell thickness, and the revered core–shell structure (reproduced from Raja et al. [113], Copyright 2016, with permission from the Royal Society of Chemistry). **b** Coaxial bioprinting and a direct bioprinting strategy combined with sacrificial bioprinting (reproduced from Shao et al. [118], Copyright 2020, with permission from IOP Publishing). **c** Schematic diagram and SEM image of the internal drug-carrying scaffold (reproduced from Li et al. [120], Copyright 2019, with permission from the authors)

adjusted to form a triangular pore shape. The triangles make up for the insufficient mechanical properties of AlgGG and increase the overall stability [124] The modified scaffold contributes to a significant increase in the branching of the vascular network and a substantial rise in the total tubular length.

Lotus seedpod-like structure (Fig. 6b): The structure of the lotus house is simulated to create a scaffold wrapped in "lotus seeds" [125]. Similar to the seed shapes, hydrogel microspheres encapsulating deferoxamine (DFO) liposomes can be injected directly into the 3D-printed bioceramic scaffold. These microspheres account for building internal vascularization. The "lotus seedpod"-shaped β-tricalcium phosphate (β-TCP) scaffold provides mechanical support, and preforms the osteogenic region. The bioceramic material serves as an effective material for osteogenesis, whereas it requires high-temperature sintering, often inactivating the loading factor. Nonetheless, the separation of "lotus seeds" and "lotus seedpod" avoids this situation, expanding the application range of bioceramic materials.

As mentioned above, regardless of the source of structural design, the result is the separation of osteogenic and angiogenic regions. The most significant advantage of sub-regional scaffolds is that different regions can be printed into different materials based on various characteristics, while different factors can be loaded onto them. Materials meeting both bone and vascular regeneration requirements have been rare, while combining different materials is an easier approach. Those exhibiting high mechanical strength are selected for the osteogenesis region. On the other hand, soft materials that can load fragile factors can more significantly contribute to the regeneration of blood vessels. When the two regions are treated separately, it can protect the active ingredients to the greatest extent, thereby eliminating numerous limitations of porous scaffolds. This suggests that sub-regional scaffolds have double stimulation factors to facilitate angiogenesis, and allow revascularization to be achieved more effectively.

Tubular scaffolds

The design of osteogenesis grafts that facilitate vascularization has one feature in common: they enable the graft core to communicate with the host as efficiently as possible. As a basis for integration, rapid communication avoids the occurrence of graft necrosis. Accordingly, the tubular structure was

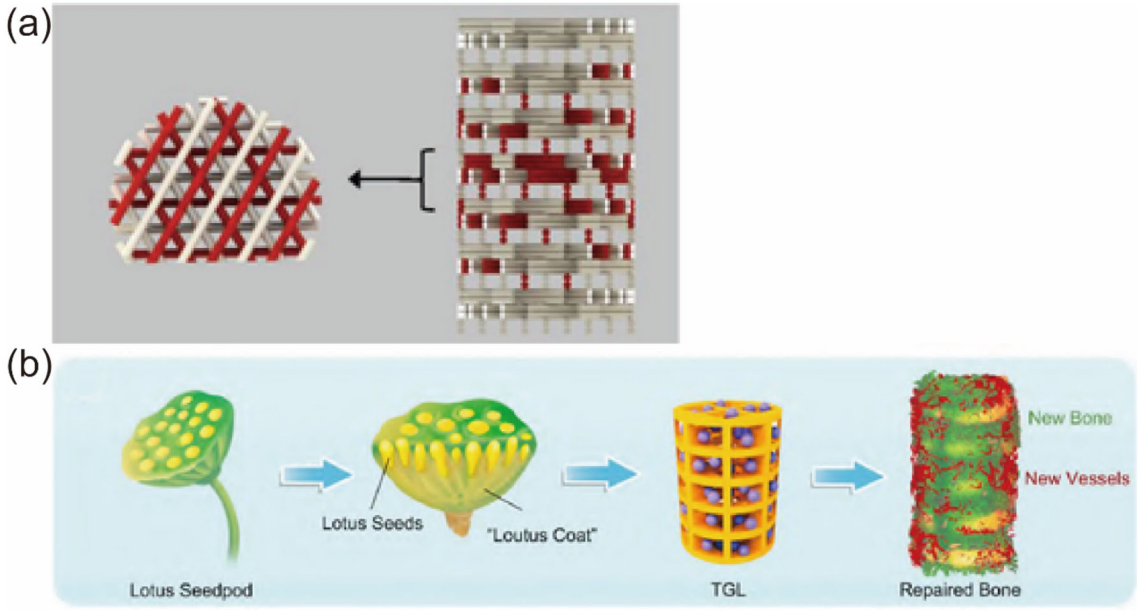

Fig. 6 **a** Schematic illustration of the olive-shaped scaffold with top and longitudinal views. The white color indicates calcium phosphate cement (CPC) and the red color indicates alginate–gellan gum (AlgGG) (reproduced from Ahlfeld et al. [122], Copyright 2019, with permission from WILEY-VCH Verlag GmbH & Co. KGaA, Weinheim). **b** An inspirational lotus seedpod, and the scaffold schematic (reproduced from Han et al. [125], Copyright 2020, with permission from the authors)

gradually incorporated into graft designs. Since the development of hot dog-like structure above, the structural design of 3D-printed osteogenic grafts has been shifting to tubular structures. However, they still retain some repetitive unit characteristics and achieve the separation of the two regions, and are therefore still classified as sub-regional scaffolds.

Single tubular structure

The fabrication of a long tubular structure would be too simple to be satisfactory. In fact, it has been difficult to vascularize the central region using traditional materials, which challenge has remained [126]. A centrally vascularized tissue-engineered bone graft with a unique core–shell composite structure can solve the above problem by the side groove structure [40]. The shell portion uses β-TCP to provide mechanical support and an osteogenic matrix for bone regeneration (Fig. 7a), and the core part uses a collagen hydrogel-based bioink. The ink is internally encapsulated with endothelial colony-forming cells (ECFCs) and mesenchymal stromal cells (MSCs) to form endogenous vessels [127, 128]. Since the shell portion has a high density and long diameter, it is difficult for external vessels to extend through the shell into the core region [129]. The lateral groove structure provides a pathway for vascular invasion, which allows the central area to easily communicate with the surrounding muscle tissue at an early stage. In this way, the oxygen supply and metabolic demand of the entire core region are ensured. Internally generated vessels meet the externally wrapped vessels at the side groove. The result is a unique taco-like vascular network structure thoroughly infiltrating and perfusing the scaffold. After quantitative analysis, it was proved that the side groove can nearly double the number of vascular regenerations of the scaffold. Using this approach, complete revascularization is achieved rapidly. Similar to the aforementioned structure is the 3D-printed scaffold with a groove to incorporate the axial vascular pedicle (Fig. 7b) [130]. The introduction of blood vessels accompanying the backbone in the scaffold ensures metabolic demand within the whole segment. Besides, new capillaries can be generated to infiltrate the graft and achieve early bone replacement. This is synonymous with the current clinical use of grafts carrying vascular tissue [35]. At the same time, it avoids the secondary damage arising from extracting tissue with high vessel organization.

Multiple tubular structures

The existence of single tubular structures makes it evident that there are multiple tubular structures. The periphery of the defect site takes the lion's share of the stress in a single tubular structure. However, this does not favor the integration of the graft and the regeneration of bone tissue. Stress is of critical significance to the overall stiffness and structural integrity of nascent bone tissue, and it also affects the development of the vasculature, which partially explains why grafts made of metal are gradually falling into disfavor

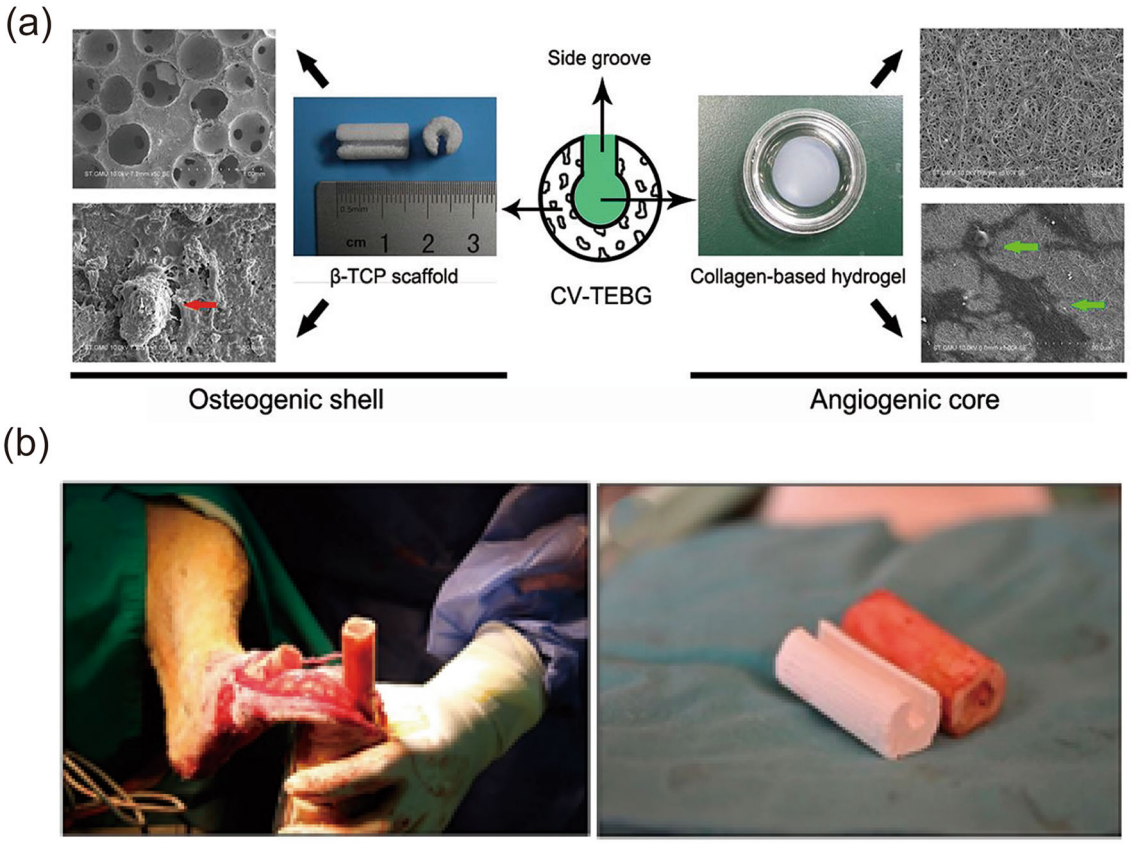

Fig. 7 **a** Osteogenic shell and angiogenic core characterized by SEM imaging, and schematic of centrally vascularized tissue engineering bone grafts (reproduced from Wang et al. [40], Copyright 2018, with permission from Elsevier). **b** Axial vascular pedicle and customized 3D-printed scaffold (reproduced from Vidal et al. [130], Copyright 2020, with permission from the authors)

[131–133]. The excessive strength and rigidity of metals tend to cause stress shielding effects, severely inhibiting tissue regeneration [134]. In contrast, multiple tubular structures allow for a more uniform distribution of stresses throughout the scaffold. They can significantly increase the specific surface area and porosity while ensuring the mechanical properties [135]. Moreover, their larger surface area can accelerate scaffold degradation and internal material release [136]. The pipelines provide space for the inward growth of the host vessel in more directions and deliver additional growth factors to the defect [137].

Plants with complex vascular systems inevitably have a "niche" in the design of tubular structures (Fig. 8a). Natural mineralized wood can directly serve as bone grafts [138]. Specifically, the fibrous vascular system native to the plant plays a vital role in the function of wood-derived bone scaffolds (Fig. 8b) [139, 140]. Biomimetic lotus root morphology scaffolds also exhibit a parallel multi-channel structure with low flow resistance (Fig. 8c) [141]. The relatively high flow rate of internal channels facilitates the distribution of oxygen and nutrients. Cells inoculated on the surface of the scaffold are promoted to actively climb to the interior of the duct at an early stage, enhancing the initial angiogenesis process in the beginning.

Moreover, the porosity, specific surface area, and mechanical strength of the scaffold can be regulated by adjusting the number of channels or the stacking approach; in this approach, the stacking significantly affects the scaffold. The hexagonal close-packed model with optimal compression resistance exhibits the lowest porosity and vice versa. However, the balance between porosity and mechanical strength should still be weighed. Also, the parametric relationship between the tube diameter and spacing affects the angiogenic effect of the scaffold [142]. Researchers have set up several experimental groups in this context. In comparison with other groups, the scaffold with spacing/diameter = 0.5/0.8 demonstrated superior angiogenesis; the vascular volumes and expression of related genes all presented high levels.

Microchannel structures

High porosity is beneficial, as revealed by the above analysis of the effect of pore size on osteogenesis and angiogenesis. On the other hand, the mechanical properties of scaffolds

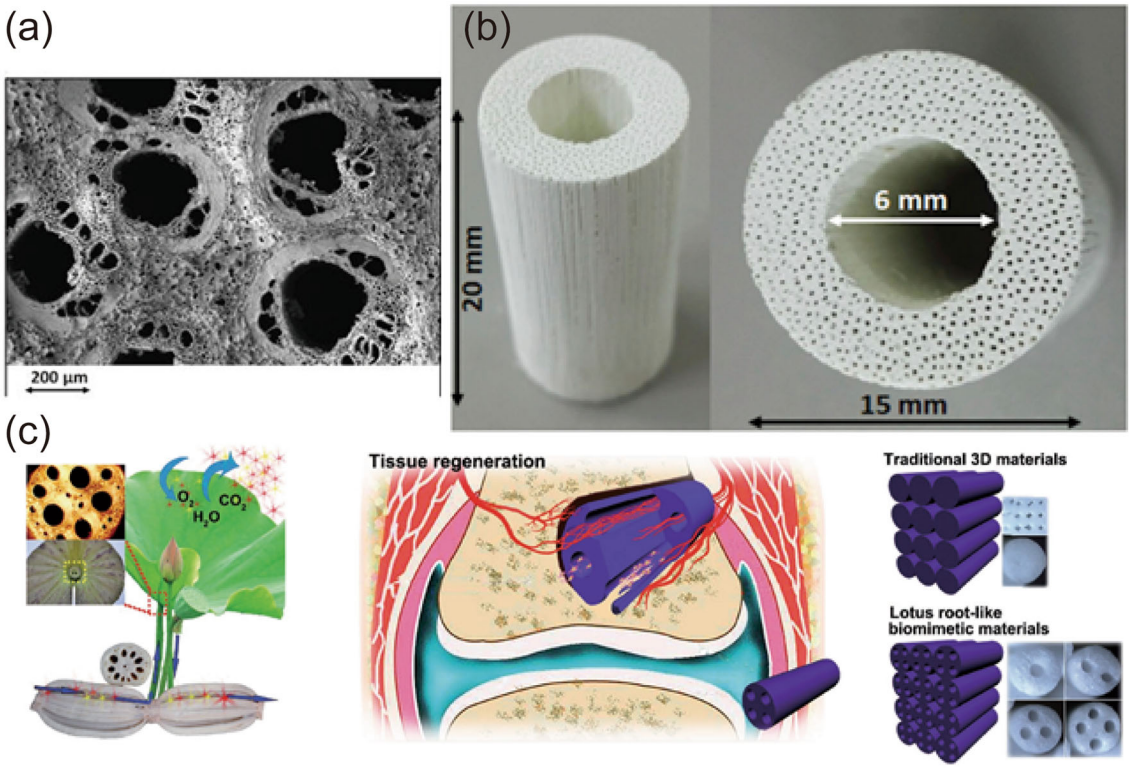

Fig. 8 **a** SEM image of the microstructure of scaffold surface after processing (reproduced from Sprio et al. [153], Copyright 2021, with permission from the authors). **b** Macroscopic images of 3D porous CaP ceramics scaffold made from natural wood (reproduced from Kon et al. [138], Copyright 2021, with permission from the authors). **c** The schematics of the lotus root microstructure, application of lotus root-like scaffold in tissue regeneration, and comparison between the biomimetic scaffold and the traditional scaffold (reproduced from Feng et al. [141], Copyright 2017, with permission from the authors)

cannot be compromised. A great solution for this challenge is the application of microchannels. While they hardly affect the general structure and mechanical strength, they can significantly increase the porosity [143]. A microchannel averages only a few tens of microns (Fig. 9a). The PCL is printed from mixed media, resulting in a considerable number of microchannels in the fibers [144]. Microchannels significantly improve the porosity and surface area of the scaffold, which might play important roles in interactions with cells under in vivo conditions. Experimental results show that through immune regulation, cell recruitment, and other processes, microchannels promote vascularization and osteogenesis. A large number of interconnected microchannels in the scaffold make the scaffold fibers appear porous and spongy, contributing to its good elasticity (Figs. 9b and 9c) [145]. The paracrine mechanism of MSC is also activated to promote angiogenesis [146].

In comparison with channels that have a diameter of hundreds of microns, the diameter of 0–50 μm enhances cell metabolism, migration, and interaction [147, 148]. Moreover, in the presence of highly interconnected microchannels, the flow rate of body fluid inside the scaffold increases dramatically [149]. Scaffolds with microchannels actively attract the rapid infiltration of blood through capillary action [150]. Furthermore, microchannels can draw cells and facilitate cell adhesion by capillary action [151]. All of these actions benefit scaffolds to achieve rapid angiogenesis. Although the preliminary results are promising, the resolution of current 3D printers is insufficient to output microchannels [152]. Hence, the above microstructures can be obtained by modifying the material of the scaffold, which can also provide a reference for the structural design of the scaffold. When the resolution is increased, the microchannels could be printed as a part of more complex and delicate scaffolds to facilitate angiogenesis.

In general, tubular scaffolds are more tailored to the truncated defects of long bones. Accordingly, the weight of mechanical properties has been strengthened in the structural design. Compared with sub-regional scaffolds, tubular scaffolds do not add new stimulation factors but aim to achieve the structural optimization of the vascular growth space. The tubes serve as the main area of vascular regeneration. As mentioned above regarding the effect of pore size in porous scaffolds, a tubular structure with a larger internal diameter

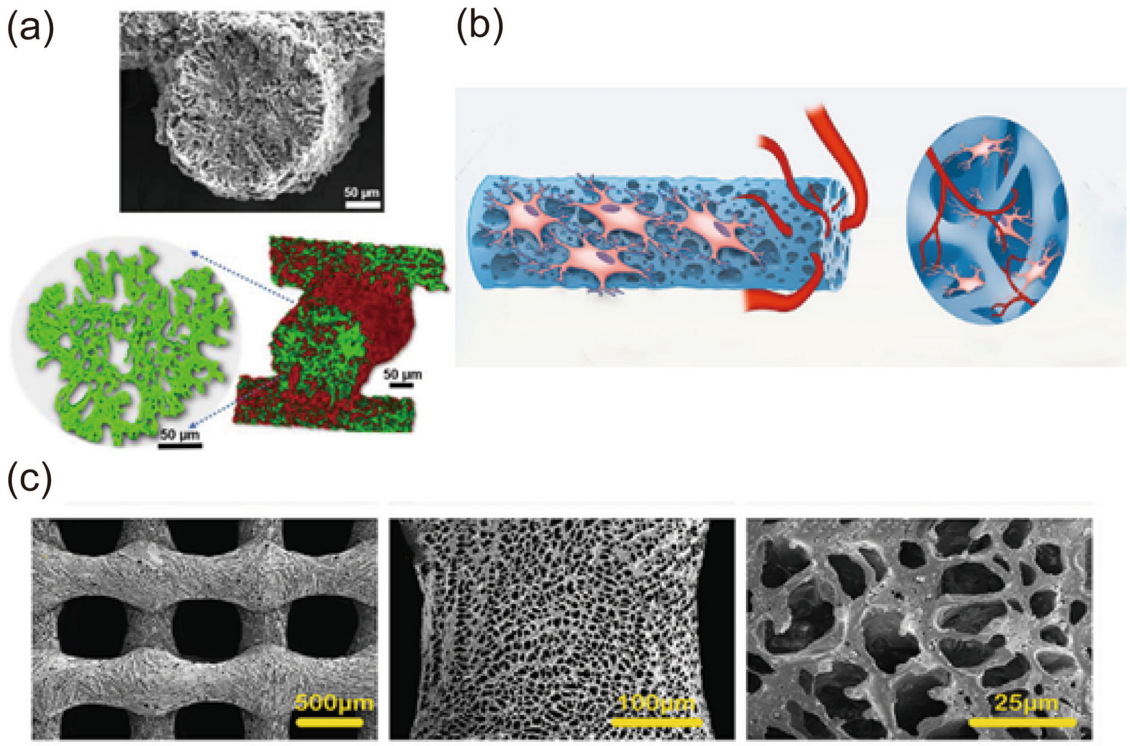

Fig. 9 **a** SEM cross-sectional image and digital image in μCh of microchannels. The red color indicates highly open channeled pores, and the green color indicates struts (reproduced from Won et al. [144], Copyright 2019, with permission from Elsevier). **b** The schemata of a spongy scaffold with microchannels, and **c** the surface SEM images of the spongy scaffold (reproduced from Lian et al. [145], Copyright 2021, with permission from Elsevier)

facilitates rapid vessel growth. Unlike the relatively complex internal spaces in other scaffolds, the straight and unobstructed interior aids the rapid exchange of substances and the invasion of blood vessels. Furthermore, when the longitudinal axis of the scaffold is excessively long, the lateral axis needs access to ensure that the center does not become necrotic. The morphology of the scaffold at this point is similar to Haversian canals, i.e., the structure responsible for blood supply inside the bone.

Bone-like scaffolds

The ultimate goal of employing 3D-printed osteogenic scaffolds is to repair large bone defects in the human body. As a result, it is highly appropriate to imitate the native bone structure. However, the human body, a product of billions of years of evolution, has a highly complex structure [153]. With the current state of technology, grafts are not capable of perfect imitation. Most of the aforementioned grafts capture limited characteristics of the native skeleton. For instance, imitation is achieved either from a macroscopic or a microscopic point of view.

Macrostructure simulations

Bone defects are usually irregular and complex in morphology [154]. Traditional graft morphology is relatively fixed and simple for easy mass production; however, the above structures do not correspond to the actual anatomy of the human body, resulting in several problems (e.g., abrasion of the integration surface and improper stress distribution) [155, 156]. All of these issues may lead to the failure of graft integration, poor prognosis, and adverse sequelae [157].

Furthermore, 3D printing, standing out for its personalized customization ability, is capable of creating grafts that can be precisely matched by mimicking the bone structure [158, 159]. Before printing, the morphological structure of the local bone is achieved by computed tomography (CT) (Figs. 10a–10e) [160–162]. In practical human applications, it is also possible to obtain relatively compatible data by scanning the symmetrical bones in the defective area. A graft effectively fitting the defect site can lead to rapid integration and early healing of the graft [163, 164].

However, this macroscopic mimicry does not have a considerable effect on the rapid regeneration of blood vessels. It can only be recognized as a refinement of the conventional graft that does not significantly enhance the regeneration,

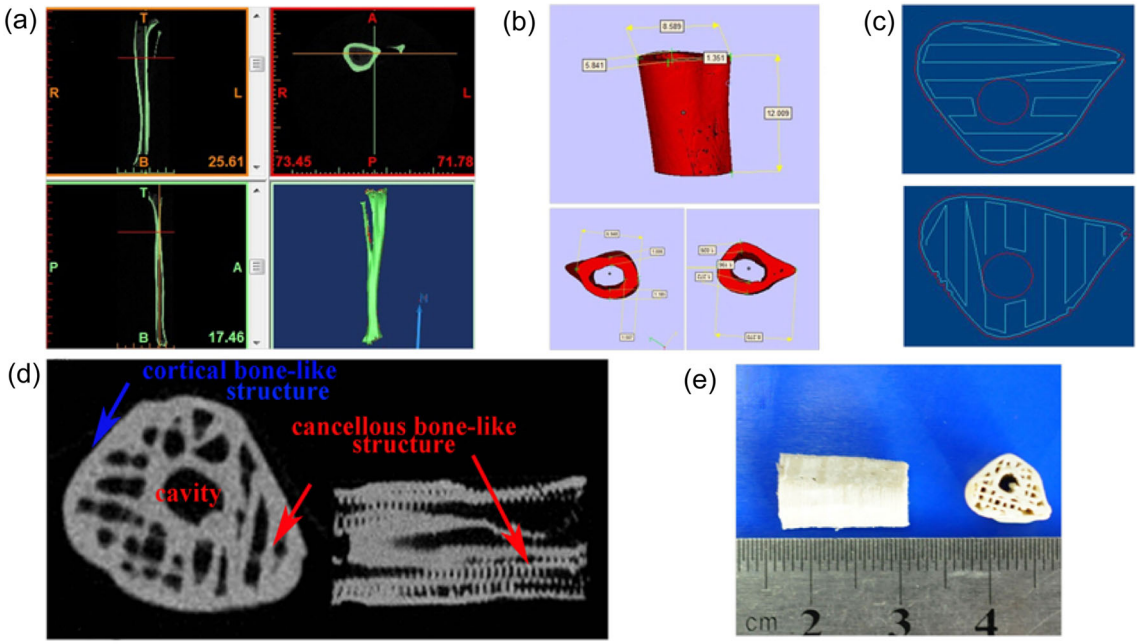

Fig. 10 **a** CT scan of rabbit leg. **b** Reconstruction of fragments. **c** The design of prints. **d**, **e** The CT scan and photograph of 3D-printed scaffolds (reproduced from Bao et al. [160], Copyright 2017, with permission from the authors)

more like an additionally modified part of the overall graft structural design.

Microstructure simulation scaffolds

The macrostructure of bones is fairly easy to imitate; it is the appropriate mimicking of bone function, i.e., microstructure, that is the critical task of bone-like scaffolds [165].

According to structure, bones can be simply divided into cortical and cancellous bones (Fig. 11a) [166]. Cancellous bone is formed by considerable interwoven bone trabeculae and appears as a loose spongy network [167]. By contrast, cortical bone sections are more intricate. Mature cortical bone consists of lamellar bone and is significantly dense [168].

Layers of bone plates wrap around in a concentric structure, encasing nerves and blood vessels, which leads to the formation of the Haversian system to nourish the bone and transmit information [169, 170]. Cortical bone and cancellous bone have such different structures that it is extremely challenging to print the two as a whole. Currently, the two scaffolds are combined using the demineralized bone matrix (DBM) instead of 3D printing [171]. In the next sections, cancellous and cortical bone scaffolds are described separately, with a focus on the more complex cortical bone that assumes more physiological functions.

Cancellous-like bone scaffolds

Cancellous-like bone scaffolds have been simulated using different well-established techniques. The loose and porous structure can be formed using 3D printing technology, supercritical carbon dioxide ($scCO_2$) foaming technique, electron beam melting (EBM), and other methods [172, 173]. Although 3D printing allows for more accurate control of the internal structure, in comparison with other technologies, porous scaffolds are still directly used as cancellous bone [174]. As a result, most of the existing cancellous-like bone scaffolds do not fully conform to the anatomical and physiological characteristics of cancellous bone [175]. The main reason is that the arrangement of trabeculae is not disorderly or somewhat regular but changes according to the stress of the bone, which requires scaffolds that are mechanically adaptive.

Cortical-like bone scaffolds

The most distinctive feature of cortical bones is the Haversian system, which consists of Haversian and Volkmann canals that maintain the blood supply. Accordingly, the Haversian system architecture is the most critical component of a cortical-like bone scaffold. Thus, a bone-like scaffold interface is concentric circle-like, with a central area simulating cancellous bone [176]. Haversian canals are tubular channels arranged in the peripheral part of the scaffold, which are interconnected by a ring of Volkmann canals (Fig. 11b). Similar

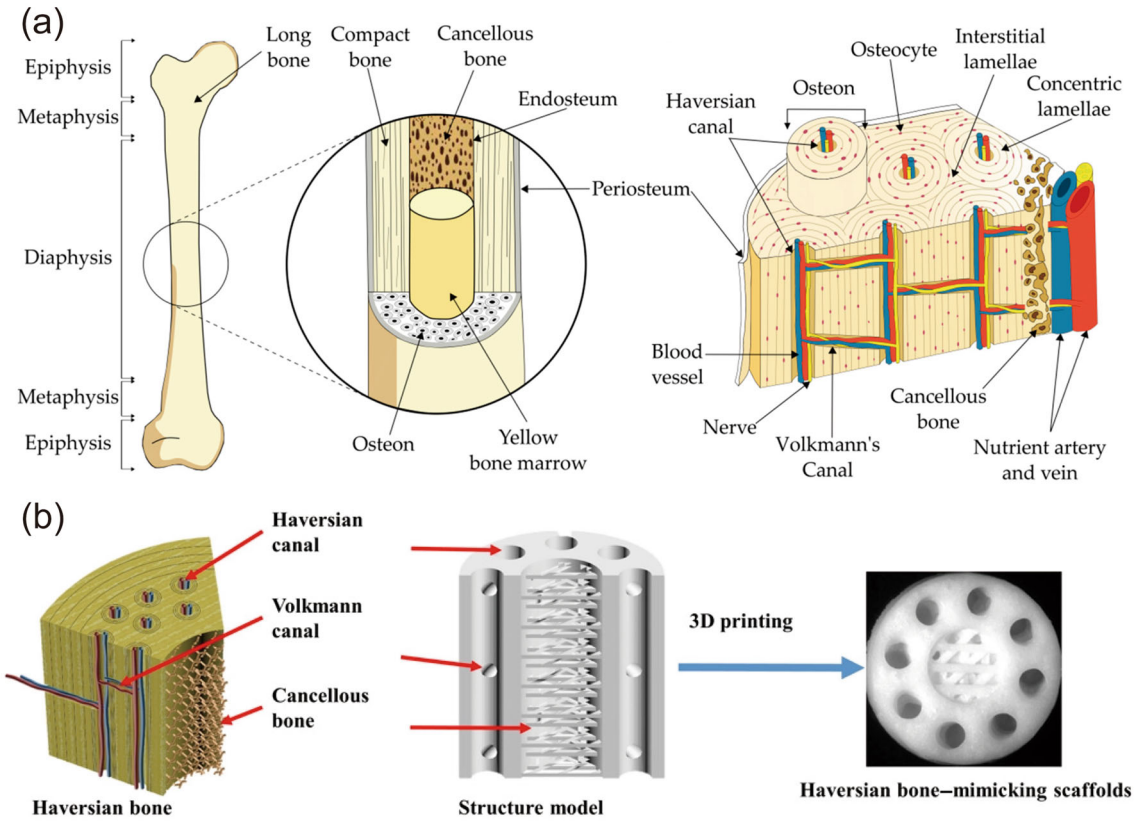

Fig. 11 **a** Composition of long bone and its microstructure (reproduced from Robles-Linares et al. [166], Copyright 2019, with permission from the authors). **b** The schemata of Haversian canals, Volkmann canals, and cancellous bone, corresponding structural model, as well as 3D-printed Haversian bone–mimicking scaffolds (reproduced from Zhang et al. [176], Copyright 2020, with permission from the authors)

to the above lotus root mimic structure, the mechanical properties of the grafts can be regulated to optimally match to the host by adjusting the number and diameter of tubes. Moreover, the scaffold can specifically load different cells in each region [177]. Osteoblasts are inoculated in the cancellous bone fraction and angiogenic cells are inoculated in the vascular channels to develop a non-contact co-culture system. Existing studies have demonstrated that a proper distance between multiple cells can maintain their mutual synergistic effects, since it provides a better environment for the respective proliferation and differentiation of cells [127, 178].

Unlike the increasingly refined simulation of Haversian and Volkmann canals, they have also been simplified in other approaches. The current 3D printing technology has made it possible to produce osteogenic grafts integrating an actual functional vascular system [18, 165]. However, its relative resolution and fineness are still insufficient [179]. Besides, the voids created during direct printing may cause structural deformation [180, 181]. Another option is to print the vascular system first with sacrificial Pluronic inks (Fig. 12a) [182]. Subsequently, this can be wrapped by a GelMA hydrogel loaded with MSC. Next, the sacrificial material is removed immediately to obtain a GelMA scaffold with the vascular pathway formed (Fig. 12b) [183]. New blood vessels grow rapidly to the core of the graft through the designed vascular structure, which ensures the growth of cells and avoids the occurrence of central necrosis. Moreover, the overall level of vascularization and osteogenesis in scaffolds with vascular structures is significantly increased due to the rapid communication. The grafts are also easier to degrade and replace as a result of the presence of channels. If the graft fails to decompose, it would occupy space and inhibit bone regeneration [184].

The Haversian system is made up of Haversian canals and bone plates, which is also a bone unit called the osteon. Unlike the scaffolds above, those discussed below focus on a single bone unit rather than a unitary vascular structure. High mechanical strength PCL serves as the support carrier, and it is printed to form a concentric three-ring structure [185]. The outermost loop and the central loop act as the supporting skeleton, and the middle loop is hollowed out (Fig. 13a). The central loop fulfills the function of cancellous bone. Four osteon-like units surround the central area in the middle loop. The osteon-like unit shows a concentric ring

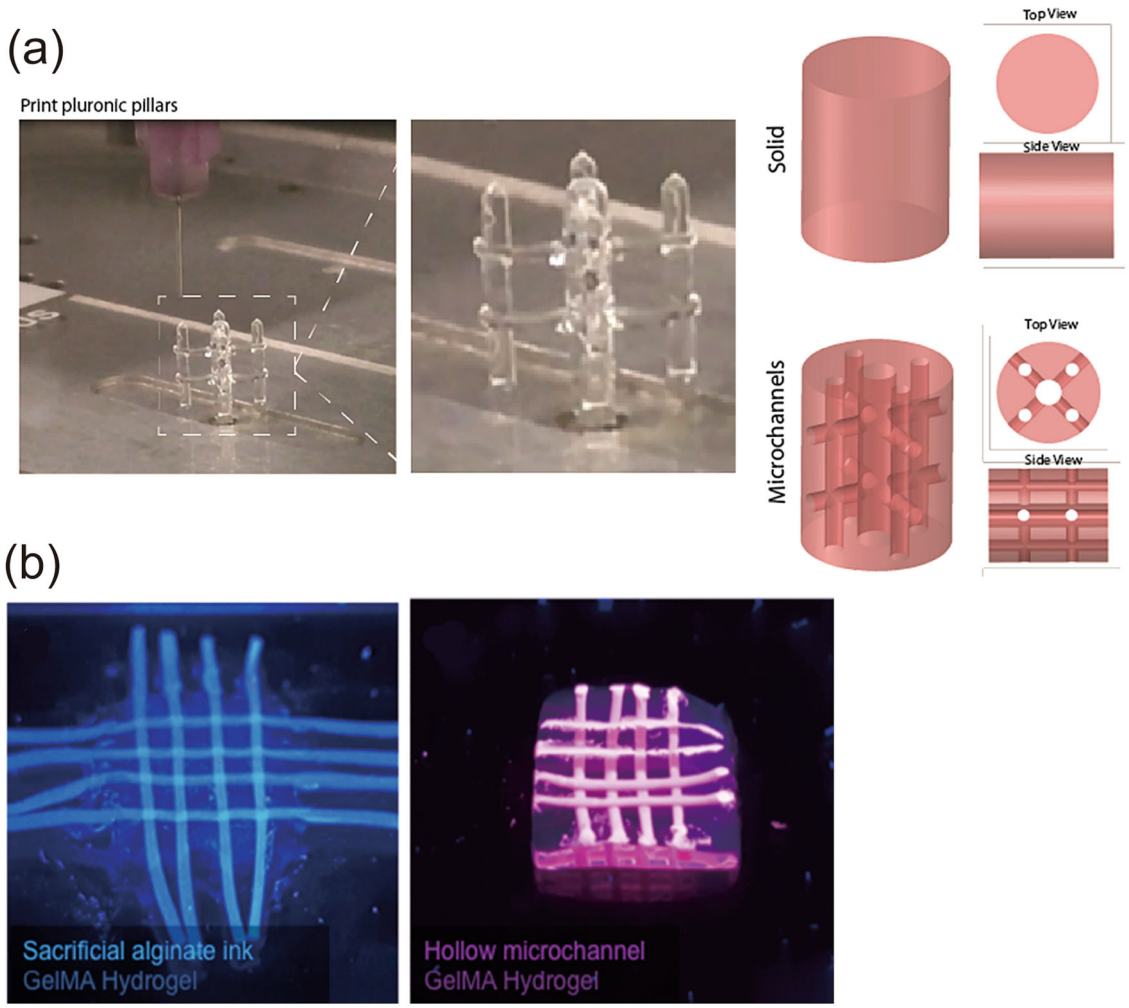

Fig. 12 **a** Printed sacrificial Pluronic micropillars as well as the solid and microchannels with top and side views, demonstrating interconnected microchannel networks within the constructs (reproduced from Daly et al. [182], Copyright 2018, with permission from Elsevier). **b** Integral scaffold before sacrificial ink removal and scaffold with complete vascular structure (reproduced from Twohig et al. [183], Copyright 2021, with permission from Elsevier)

structure, and it is printed with a composite hydrogel composed of cell-loaded fibrinogen and gelatin. Its outermost ring is loaded with MSCs for osteogenesis, thus forming the bone plate structure. Meanwhile, the innermost ring is loaded with human umbilical vascular endothelial cells (HUVECs) for vascularization. When compared with cast samples without structure, no significant difference was found in the expression of osteogenic marker genes in the printed samples (Fig. 13b). A significant change can be identified in the angiogenic marker mRNA, which is several-fold higher. The structural design was demonstrated to significantly facilitate angiogenesis. A block biomimetic scaffold comprises a composite hydrogel, which also simulates osteon-like units [186]. Unlike the one discussed earlier, this scaffold abandons the external support skeleton and focuses on exploring the simulation of osteon-like units (Fig. 13c). The unit blocks are concentric double-ring structures. The inner ring mimics vascular tubules and encapsulates HUVECs, while the outer ring acts as part of the bone encapsulating human osteoblast-like cells (MG63s). The integral support is formed by stacking plural die blocks as a long cylinder with an internal tube cavity, and the assembly provides better mechanical properties. As revealed by experiments, the assembly shows higher expression of the vascular-related gene VEGF in comparison with the individual osteon-like units, which confirms the importance of the lumen structure.

The bone-like scaffolds are further optimized based on the above scaffolds, which makes them approach the physiological state of human beings. However, the simplified simulation for the vascular system is more adapted to the current production level to scale up and expand the production. On the one hand, scaffolds that can withstand stress and have an ade-

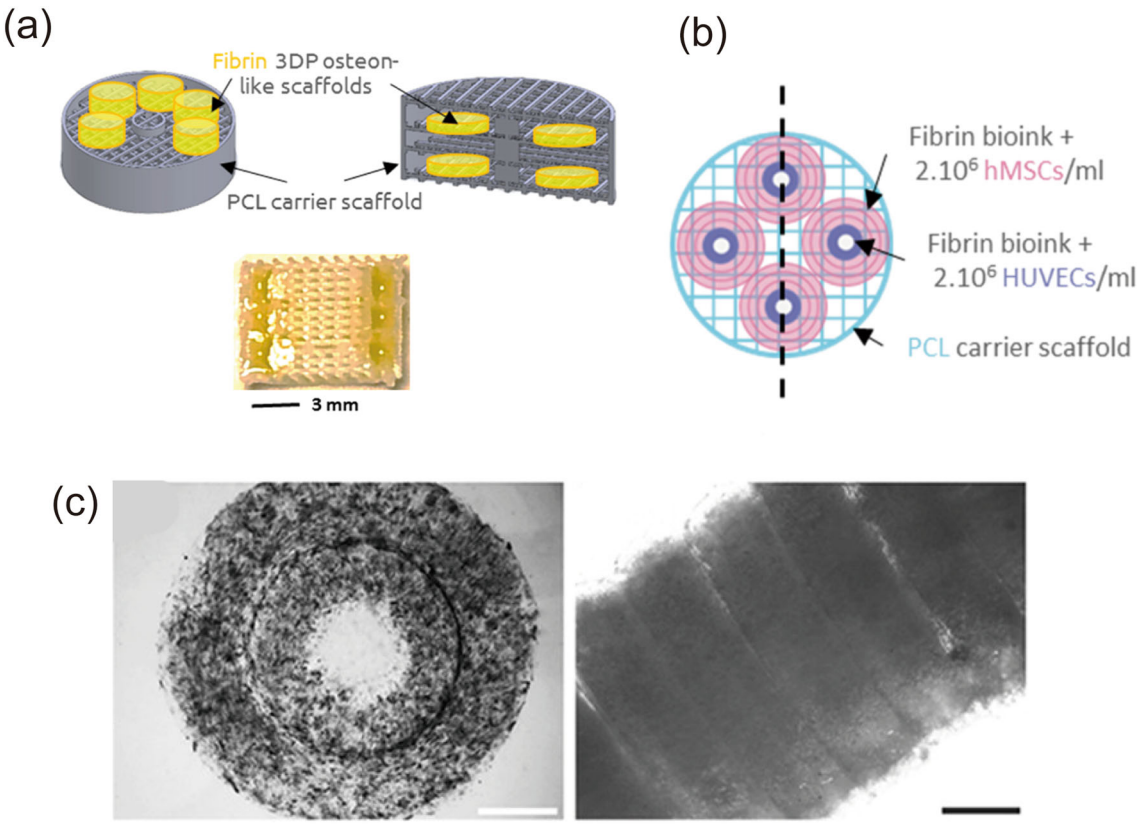

Fig. 13 **a** Schematic of 3D printed scaffolds. The green color represents osteon-like units and the gray represents a polycaprolactone (PCL) carrier scaffold. Micrograph of the 3D printed scaffold. **b** Schematic of the 3D-printed scaffolds (top view). Each layer comprises four osteon-like fibrin hydrogels. Each osteon-like unit consists of four rings with different cells (reproduced from Piard et al. [185], Copyright 2019, with permission from IOP Publishing). **c** The osteon-like double-ring modules: phase-contrast images of a single unit and an assembly. Scale bar = 500 μm (reproduced from Zuo et al. [186], Copyright 2015, with permission from American Chemical Society)

quate and appropriate vascular growth network can be used as simple substitutes for natural bone. On the other hand, composite scaffolds with elaborate structures should be the goal that researchers strive for in the future. The functional structure of cortical bone can be met by incorporating sclerotin with canals on the whole. Subsequently, the cancellous bone is combined with cortical bone scaffolds. A bone-like scaffold displaying the same natural bone structure can be formed, which takes on most of the functions of the original tissue while inducing the complete regeneration of real bone tissue.

Conclusions and prospects

Achieving rapid vascularization is recognized as a vital step in bone tissue engineering. In comparison with the direct regeneration of vascular tissue, vascularization in bone exhibits its specificities. Importantly, the hole graft should meet the requirements of osteogenesis and exhibit sufficient mechanical properties. 3D-printed osteogenic grafts allow for the construction of specific structures that meet their characteristics while allowing for the rapid establishment of a blood supply. Current 3D-printed grafts are combined by multiple methods that work together to facilitate rapid vascularization. As a foundation scaffold, the best conceivable, biomimetic, ergonomic structure is one that enables the scaffold to incorporate all vital functions.

In general, any scaffold requires vascularized areas or appropriate vascular growth pathways; only through the apposite space can blood vessels invade and grow as well as provide the means for communication between the graft and the host. In other words, maximum vascular regeneration can only be achieved by biomimetic channels. Although a porous scaffold is easy to print and is universal, its internal structure makes it difficult to precisely control the travel area of blood vessels. Above all, scaffolds are required that can be precisely controlled; in this regard, the biomimetic tubular scaffold is currently the superior choice, as it can be more conveniently connected with the host's vascular system to achieve early perfusion. At present, the diameter, density, and form of the channels can be adjusted through 3D print-

ing. Besides, it has been shown in animal models that refining the above parameters achieves the desired effect of rapid vascularization. Overall, 3D-printed grafts are characterized by fewer complications, faster integration of the graft, and earlier complete regeneration of bone tissue.

The biomimetic tubular scaffold presents several advantages in mass production and clinical transformation; yet we still need to develop complete imitations of natural bones using 3D scaffolds. As already attempted in the microstructure simulation scaffolds above, different tissue-forming regions are also reproduced in the bone-like scaffold. Natural bone tissue is the composite product of multiple components and cells. Among them, blood vessels account for a vital part of osteogenesis, albeit other structures are also important, such as nerves accompanying and nourishing the bones through the Haversian canal. Accordingly, when designing the scaffolds, it is also possible to consider innervation. As a result, bone-like scaffolds can feature a multi-layered physical structure; such complex architectures are a prerequisite for achieving the spatial distribution of multiple cell types. Furthermore, a structure conducive to cell-specific distribution will be more capable of regulating the interactions between various cells and generating specialized tissues. This avoids the structural disorganization of regenerating tissues, reduces tumor production, and shortens the time for late remodeling and repair by the host itself.

Moreover, different parts of the scaffold are assembled together with their corresponding functional materials. Similar to the interactions between cells and tissues during the growth, maintenance, and repair of bone, the interactions between the components within the 3D-printed bone-like scaffold should also be meticulously considered. Given these important aspects, the understanding of bone regeneration mechanisms is still incomplete. Therefore, the challenge to increase the simulation specificity of the bone structure as described above is an urgent problem that needs to be addressed. Since biomimetics encompass many definitions, we cannot restrict ourselves to simulations of physical and chemical aspects. Accordingly, biologically plausible mimicry for osteogenesis has been developed. Taking exosomes as an example, cells communicate with each other via exosomes. Therefore, scaffolds with exosomes can be regarded as those with intercomponent regulation, which is another future exploration direction of bone tissue engineering.

At the same time, the resolution of the 3D printer is highly important. Given the general understanding of bone regeneration, for now, the current 3D printer resolution is inadequate to meet the requirements. A nano-scale 3D printer with ultra-high resolution would be needed to print an osteogenic scaffold that meets our vision. 3D bioprinting, which is currently the most promising technology to produce complex transplants, should strive to facilitate its research development goals, achieve clinical translation as soon as possible, and bring more benefits to people in need.

Acknowledgements This research is supported by the Zhejiang Province Key Research and Development Program (No. 2021C03059).

Author contributions WL was involved in conceptualization, investigation, writing—original draft, writing—review and editing, and visualization; YS was involved in writing—review and editing; ZX was involved in supervision.

Declarations

Conflict of interest The authors declare that they have no conflict of interest.

Ethical approval No studies with human or animal subjects were conducted afresh by the authors for inclusion in this review article.

References

1. Wu V, Helder MN, Bravenboer N et al (2019) Bone tissue regeneration in the oral and maxillofacial region: a review on the application of stem cells and new strategies to improve vascularization. Stem Cells Int 2019:6279721. https://doi.org/10.1155/2019/6279721
2. Zhang L, Yang G, Johnson BN et al (2019) Three-dimensional (3D) printed scaffold and material selection for bone repair. Acta Biomater 84:16–33. https://doi.org/10.1016/j.actbio.2018.11.039
3. Buyuksungur S, Tanir TE, Buyuksungur A et al (2017) 3D printed poly(ε-caprolactone) scaffolds modified with hydroxyapatite and poly(propylene fumarate) and their effects on the healing of rabbit femur defects. Biomater Sci 5(10):2144–2158. https://doi.org/10.1039/c7bm00514h
4. Sutradhar A, Paulino GH, Miller MJ et al (2010) Topological optimization for designing patient-specific large craniofacial segmental bone replacements. Proc Natl Acad Sci USA 107(30):13222–13227. https://doi.org/10.1073/pnas.1001208107
5. Bhumiratana S, Bernhard JC, Alfi DM et al (2016) Tissue-engineered autologous grafts for facial bone reconstruction. Sci Transl Med 8(343):343ra83. https://doi.org/10.1126/scitranslmed.aad5904
6. Shahabipour F, Ashammakhi N, Oskuee RK et al (2020) Key components of engineering vascularized 3-dimensional bioprinted bone constructs. Transl Res 216:57–76. https://doi.org/10.1016/j.trsl.2019.08.010
7. Amiryaghoubi N, Fathi M, Pesyan NN et al (2020) Bioactive polymeric scaffolds for osteogenic repair and bone regenerative medicine. Med Res Rev 40(5):1833–1870. https://doi.org/10.1002/med.21672
8. Zhang ZY, Teoh SH, Chong MS et al (2010) Neo-vascularization and bone formation mediated by fetal mesenchymal stem cell tissue-engineered bone grafts in critical-size femoral defects. Biomaterials 31(4):608–620. https://doi.org/10.1016/j.biomaterials.2009.09.078
9. Freeman FE, Mcnamara LM (2017) Endochondral priming: a developmental engineering strategy for bone tissue regeneration. Tissue Eng Part B Rev 23(2):128–141. https://doi.org/10.1089/ten.TEB.2016.0197

10. Myeroff C, Archdeacon M (2011) Autogenous bone graft: donor sites and techniques. J Bone Joint Surg Am 93(23):2227–2236. https://doi.org/10.2106/JBJS.J.01513
11. Omar O, Engstrand T, Linder LKB et al (2020) In situ bone regeneration of large cranial defects using synthetic ceramic implants with a tailored composition and design. Proc Natl Acad Sci USA 117(43):26660–26671. https://doi.org/10.1073/pnas.2007635117
12. Agarwal R, García AJ (2015) Biomaterial strategies for engineering implants for enhanced osseointegration and bone repair. Adv Drug Deliv Rev 94:53–62. https://doi.org/10.1016/j.addr.2015.03.013
13. Tomlinson RE, Silva MJ (2013) Skeletal blood flow in bone repair and maintenance. Bone Res 1(4):311–322. https://doi.org/10.4248/BR201304002
14. Stegen S, van Gastel N, Carmeliet G (2015) Bringing new life to damaged bone: the importance of angiogenesis in bone repair and regeneration. Bone 70:19–27. https://doi.org/10.1016/j.bone.2014.09.017
15. Einhorn TA, Gerstenfeld LC (2015) Fracture healing: mechanisms and interventions. Nat Rev Rheumatol 11(1):45–54. https://doi.org/10.1038/nrrheum.2014.164
16. Hankenson KD, Dishowitz M, Gray C et al (2011) Angiogenesis in bone regeneration. Injury 42(6):556–561. https://doi.org/10.1016/j.injury.2011.03.035
17. Mercado-Pagan AE, Stahl AM, Shanjani Y et al (2015) Vascularization in bone tissue engineering constructs. Ann Biomed Eng 43(3):718–729. https://doi.org/10.1007/s10439-015-1253-3
18. Cui H, Zhu W, Holmes B et al (2016) Biologically inspired smart release system based on 3D bioprinted perfused scaffold for vascularized tissue regeneration. Adv Sci 3(8):1600058. https://doi.org/10.1002/advs.201600058
19. Kang HW, Lee SJ, Ko IK et al (2016) A 3D bioprinting system to produce human-scale tissue constructs with structural integrity. Nat Biotechnol 34(3):312–319. https://doi.org/10.1038/nbt.3413
20. Park YL, Park K, Cha JM (2021) 3D-bioprinting strategies based on in situ bone-healing mechanism for vascularized bone tissue engineering. Micromachines 12(3):287. https://doi.org/10.3390/mi12030287
21. He Y, Wang W, Lin S et al (2022) Fabrication of a bio-instructive scaffold conferred with a favorable microenvironment allowing for superior implant osseointegration and accelerated in situ vascularized bone regeneration via type H vessel formation. Bioact Mater 9:491–507. https://doi.org/10.1016/j.bioactmat.2021.07.030
22. Griffith CK, Miller C, Sainson RC et al (2005) Diffusion limits of an in vitro thick prevascularized tissue. Tissue Eng 11(1–2):257–266. https://doi.org/10.1089/ten.2005.11.257
23. Alcala-Orozco CR, Cui X, Hooper GJ et al (2021) Converging functionality: strategies for 3D hybrid-construct biofabrication and the role of composite biomaterials for skeletal regeneration. Acta Biomater 132:188–216. https://doi.org/10.1016/j.actbio.2021.03.008
24. Xing F, Xiang Z, Rommens PM et al (2020) 3D bioprinting for vascularized tissue-engineered bone fabrication. Materials 13(10):2278. https://doi.org/10.3390/ma13102278
25. Tsigkou O, Pomerantseva I, Spencer JA et al (2010) Engineered vascularized bone grafts. Proc Natl Acad Sci USA 107(8):3311–3316. https://doi.org/10.1073/pnas.0905445107
26. Zhang YS, Oklu R, Dokmeci MR et al (2018) Three-dimensional bioprinting strategies for tissue engineering. Cold Spring Harb Perspect Med 8(2):a025718. https://doi.org/10.1101/cshperspect.a025718
27. Lee H, Jang TS, Han G et al (2021) Freeform 3D printing of vascularized tissues: challenges and strategies. J Tissue Eng 12:20417314211057236. https://doi.org/10.1177/20417314211057236
28. Zhang Y, Kumar P, Lv S et al (2021) Recent advances in 3D bioprinting of vascularized tissues. Mater Des 199:109398. https://doi.org/10.1016/j.matdes.2020.109398
29. Barba A, Maazouz Y, Diez-Escudero A et al (2018) Osteogenesis by foamed and 3D-printed nanostructured calcium phosphate scaffolds: effect of pore architecture. Acta Biomater 79:135–147. https://doi.org/10.1016/j.actbio.2018.09.003
30. de Grado GF, Keller L, Idoux-Gillet Y et al (2018) Bone substitutes: a review of their characteristics, clinical use, and perspectives for large bone defects management. J Tissue Eng 9:2041731418776819. https://doi.org/10.1177/2041731418776819
31. Vidal L, Kampleitner C, Brennan MA et al (2020) Reconstruction of large skeletal defects: current clinical therapeutic strategies and future directions using 3D printing. Front Bioeng Biotechnol 8:61. https://doi.org/10.3389/fbioe.2020.00061
32. Yin S, Zhang W, Zhang Z et al (2019) Recent advances in scaffold design and material for vascularized tissue-engineered bone regeneration. Adv Healthc Mater 8(10):e1801433. https://doi.org/10.1002/adhm.201801433
33. Vidal L, Brennan MA, Krissian S et al (2020) In situ production of pre-vascularized synthetic bone grafts for regenerating critical-sized defects in rabbits. Acta Biomater 114:384–394. https://doi.org/10.1016/j.actbio.2020.07.030
34. Kawai T, Pan CC, Okuzu Y et al (2021) Combining a vascular bundle and 3D printed scaffold with BMP-2 improves bone repair and angiogenesis. Tissue Eng Part A 27(23–24):1517–1525. https://doi.org/10.1089/ten.TEA.2021.0049
35. Wang L, Fan H, Zhang ZY et al (2010) Osteogenesis and angiogenesis of tissue-engineered bone constructed by prevascularized β-tricalcium phosphate scaffold and mesenchymal stem cells. Biomaterials 31(36):9452–9461. https://doi.org/10.1016/j.biomaterials.2010.08.036
36. Cicha I, Detsch R, Singh R et al (2017) Biofabrication of vessel grafts based on natural hydrogels. Curr Opin Biomed Eng 2:83–89. https://doi.org/10.1016/j.cobme.2017.05.003
37. Chlupac J, Filova E, Bacakova L (2009) Blood vessel replacement: 50 years of development and tissue engineering paradigms in vascular surgery. Physiol Res 58(Suppl 2):S119–S140. https://doi.org/10.33549/physiolres.931918
38. Li B, Ruan C, Ma Y et al (2018) Fabrication of vascularized bone flaps with sustained release of recombinant human bone morphogenetic protein-2 and arteriovenous bundle. Tissue Eng Part A 24(17–18):1413–1422. https://doi.org/10.1089/ten.TEA.2018.0002
39. Kaempfen A, Todorov A, Guven S et al (2015) Engraftment of prevascularized, tissue engineered constructs in a novel rabbit segmental bone defect model. Int J Mol Sci 16(6):12616–12630. https://doi.org/10.3390/ijms160612616
40. Wang L, Zhu LX, Wang Z et al (2018) Development of a centrally vascularized tissue engineering bone graft with the unique core-shell composite structure for large femoral bone defect treatment. Biomaterials 175:44–60. https://doi.org/10.1016/j.biomaterials.2018.05.017
41. Zhou M, Yang X, Li S et al (2021) Bioinspired channeled, rhBMP-2-coated β-TCP scaffolds with embedded autologous vascular bundles for increased vascularization and osteogenesis of prefabricated tissue-engineered bone. Mater Sci Eng C Mater Biol Appl 118:111389. https://doi.org/10.1016/j.msec.2020.111389
42. Li T, Peng M, Yang Z et al (2018) 3D-printed IFN-γ-loading calcium silicate-β-tricalcium phosphate scaffold sequentially activates M1 and M2 polarization of macrophages to promote vascularization of tissue engineering bone. Acta Biomater 71:96–107. https://doi.org/10.1016/j.actbio.2018.03.012

43. Pizzicannella J, Diomede F, Gugliandolo A et al (2019) 3D printing PLA/gingival stem cells/ EVs upregulate miR-2861 and -210 during osteoangiogenesis commitment. Int J Mol Sci 20(13):3256. https://doi.org/10.3390/ijms20133256
44. Longoni A, Li J, Lindberg GCJ et al (2021) Strategies for inclusion of growth factors into 3D printed bone grafts. Essays Biochem 65(3):569–585. https://doi.org/10.1042/EBC20200130
45. Chen S, Shi Y, Zhang X et al (2020) Evaluation of BMP-2 and VEGF loaded 3D printed hydroxyapatite composite scaffolds with enhanced osteogenic capacity in vitro and in vivo. Mater Sci Eng C Mater Biol Appl 112:110893. https://doi.org/10.1016/j.msec.2020.110893
46. Min Q, Liu J, Yu X et al (2019) Sequential delivery of dual growth factors from injectable chitosan-based composite hydrogels. Mar Drugs 17(6):365. https://doi.org/10.3390/md17060365
47. Ker ED, Chu B, Phillippi JA et al (2011) Engineering spatial control of multiple differentiation fates within a stem cell population. Biomaterials 32(13):3413–3422. https://doi.org/10.1016/j.biomaterials.2011.01.036
48. Carragee EJ, Hurwitz EL, Weiner BK (2011) A critical review of recombinant human bone morphogenetic protein-2 trials in spinal surgery: emerging safety concerns and lessons learned. Spine J 11(6):471–491. https://doi.org/10.1016/j.spinee.2011.04.023
49. Adams RH, Alitalo K (2007) Molecular regulation of angiogenesis and lymphangiogenesis. Nat Rev Mol Cell Biol 8(6):464–478. https://doi.org/10.1038/nrm2183
50. Zha Y, Li Y, Lin T et al (2021) Progenitor cell-derived exosomes endowed with VEGF plasmids enhance osteogenic induction and vascular remodeling in large segmental bone defects. Theranostics 11(1):397–409. https://doi.org/10.7150/thno.50741
51. Gugliandolo A, Fonticoli L, Trubiani O et al (2021) Oral bone tissue regeneration: mesenchymal stem cells, secretome, and biomaterials. Int J Mol Sci 22(10):5236. https://doi.org/10.3390/ijms22105236
52. Karageorgiou V, Kaplan D (2005) Porosity of 3D biomaterial scaffolds and osteogenesis. Biomaterials 26(27):5474–5491. https://doi.org/10.1016/j.biomaterials.2005.02.002
53. Guo R, Lu S, Page JM et al (2015) Fabrication of 3D scaffolds with precisely controlled substrate modulus and pore size by templated-fused deposition modeling to direct osteogenic differentiation. Adv Healthc Mater 4(12):1826–1832. https://doi.org/10.1002/adhm.201500099
54. Freeman FE, Browe DC, Nulty J et al (2019) Biofabrication of multiscale bone extracellular matrix scaffolds for bone tissue engineering. Eur Cell Mater 38:168–187. https://doi.org/10.22203/eCM.v038a12
55. Blazquez-Carmona P, Sanz-Herrera JA, Martinez-Vazquez FJ et al (2021) Structural optimization of 3D-printed patient-specific ceramic scaffolds for in vivo bone regeneration in load-bearing defects. J Mech Behav Biomed Mater 121:104613. https://doi.org/10.1016/j.jmbbm.2021.104613
56. Reinwald Y, Johal RK, Ghaemmaghami AM et al (2014) Interconnectivity and permeability of supercritical fluid-foamed scaffolds and the effect of their structural properties on cell distribution. Polymer 55(1):435–444. https://doi.org/10.1016/j.polymer.2013.09.041
57. Murphy CM, Haugh MG, O'brien FJ (2010) The effect of mean pore size on cell attachment, proliferation and migration in collagen–glycosaminoglycan scaffolds for bone tissue engineering. Biomaterials 31(3):461–466. https://doi.org/10.1016/j.biomaterials.2009.09.063
58. Xue W, Krishna BV, Bandyopadhyay A et al (2007) Processing and biocompatibility evaluation of laser processed porous titanium. Acta Biomater 3(6):1007–1018. https://doi.org/10.1016/j.actbio.2007.05.009
59. Bohner M, Loosli Y, Baroud G et al (2011) Commentary: deciphering the link between architecture and biological response of a bone graft substitute. Acta Biomater 7(2):478–484. https://doi.org/10.1016/j.actbio.2010.08.008
60. Di Luca A, Szlazak K, Lorenzo-Moldero I et al (2016) Influencing chondrogenic differentiation of human mesenchymal stromal cells in scaffolds displaying a structural gradient in pore size. Acta Biomater 36:210–219. https://doi.org/10.1016/j.actbio.2016.03.014
61. Gupte MJ, Swanson WB, Hu J et al (2018) Pore size directs bone marrow stromal cell fate and tissue regeneration in nanofibrous macroporous scaffolds by mediating vascularization. Acta Biomater 82:1–11. https://doi.org/10.1016/j.actbio.2018.10.016
62. Zhou X, Zhou G, Junka R et al (2021) Fabrication of polylactic acid (PLA)-based porous scaffold through the combination of traditional bio-fabrication and 3D printing technology for bone regeneration. Colloids Surf B Biointerf 197:111420. https://doi.org/10.1016/j.colsurfb.2020.111420
63. Qiao S, Wu D, Li Z et al (2020) The combination of multi-functional ingredients-loaded hydrogels and three-dimensional printed porous titanium alloys for infective bone defect treatment. J Tissue Eng 11:1–16. https://doi.org/10.1177/2041731420965797
64. Sun Y, Wu Q, Zhang Y et al (2021) 3D-bioprinted gradient-structured scaffold generates anisotropic cartilage with vascularization by pore-size-dependent activation of HIF1α/FAK signaling axis. Nanomedicine 37:102426. https://doi.org/10.1016/j.nano.2021.102426
65. Wang C, Xu D, Lin L et al (2021) Large-pore-size Ti6Al4V scaffolds with different pore structures for vascularized bone regeneration. Mater Sci Eng C Mater Biol Appl 131:112499. https://doi.org/10.1016/j.msec.2021.112499
66. Marrella A, Lee TY, Lee DH et al (2018) Engineering vascularized and innervated bone biomaterials for improved skeletal tissue regeneration. Mater Today 21(4):362–376. https://doi.org/10.1016/j.mattod.2017.10.005
67. Gregor A, Filova E, Novak M et al (2017) Designing of PLA scaffolds for bone tissue replacement fabricated by ordinary commercial 3D printer. J Biol Eng 11:31. https://doi.org/10.1186/s13036-017-0074-3
68. Wegst UG, Bai H, Saiz E et al (2015) Bioinspired structural materials. Nat Mater 14(1):23–36. https://doi.org/10.1038/nmat4089
69. Raymond S, Maazouz Y, Montufar EB et al (2018) Accelerated hardening of nanotextured 3D-plotted self-setting calcium phosphate inks. Acta Biomater 75:451–462. https://doi.org/10.1016/j.actbio.2018.05.042
70. Kim Y, Son KH, Lee JW (2021) Auxetic structures for tissue engineering scaffolds and biomedical devices. Materials 14(22):6821. https://doi.org/10.3390/ma14226821
71. Mirkhalaf M, Dao A, Schindeler A et al (2021) Personalized baghdadite scaffolds: stereolithography, mechanics and in vivo testing. Acta Biomater 132:217–226. https://doi.org/10.1016/j.actbio.2021.03.012
72. Bidan CM, Kommareddy KP, Rumpler M et al (2013) Geometry as a factor for tissue growth: towards shape optimization of tissue engineering scaffolds. Adv Healthc Mater 2(1):186–194. https://doi.org/10.1002/adhm.201200159
73. Knychala J, Bouropoulos N, Catt CJ et al (2013) Pore geometry regulates early stage human bone marrow cell tissue formation and organisation. Ann Biomed Eng 41(5):917–930. https://doi.org/10.1007/s10439-013-0748-z
74. Zhou X, Castro NJ, Zhu W et al (2016) Improved human bone marrow mesenchymal stem cell osteogenesis in 3D bioprinted tissue scaffolds with low intensity pulsed ultrasound stimulation. Sci Rep 6:32876. https://doi.org/10.1038/srep32876

75. Lopez-Gonzalez I, Zamora-Ledezma C, Sanchez-Lorencio MI et al (2021) Modifications in gene expression in the process of osteoblastic differentiation of multipotent bone marrow-derived human mesenchymal stem cells induced by a novel osteoinductive porous medical-grade 3D-printed poly(ε-caprolactone)/β-tricalcium phosphate composite. Int J Mol Sci 22(20):11216. https://doi.org/10.3390/ijms222011216
76. Roohani-Esfahani SI, Newman P, Zreiqat H (2016) Design and fabrication of 3D printed scaffolds with a mechanical strength comparable to cortical bone to repair large bone defects. Sci Rep 6:19468. https://doi.org/10.1038/srep19468
77. Pilia M, Guda T, Appleford M (2013) Development of composite scaffolds for load-bearing segmental bone defects. Biomed Res Int 2013:458253. https://doi.org/10.1155/2013/458253
78. Xue D, Zhang J, Wang Y et al (2019) Digital light processing-based 3D printing of cell-seeding hydrogel scaffolds with regionally varied stiffness. ACS Biomater Sci Eng 5(9):4825–4833. https://doi.org/10.1021/acsbiomaterials.9b00696
79. Wang X, Xu S, Zhou S et al (2016) Topological design and additive manufacturing of porous metals for bone scaffolds and orthopaedic implants: a review. Biomaterials 83:127–141. https://doi.org/10.1016/j.biomaterials.2016.01.012
80. Carluccio D, Xu C, Venezuela J et al (2020) Additively manufactured iron-manganese for biodegradable porous load-bearing bone scaffold applications. Acta Biomater 103:346–360. https://doi.org/10.1016/j.actbio.2019.12.018
81. Li Y, Jahr H, Lietaert K et al (2018) Additively manufactured biodegradable porous iron. Acta Biomater 77:380–393. https://doi.org/10.1016/j.actbio.2018.07.011
82. Li Y, Jahr H, Pavanram P et al (2019) Additively manufactured functionally graded biodegradable porous iron. Acta Biomater 96:646–661. https://doi.org/10.1016/j.actbio.2019.07.013
83. Hann SY, Cui H, Esworthy T et al (2021) Dual 3D printing for vascularized bone tissue regeneration. Acta Biomater 123:263–274. https://doi.org/10.1016/j.actbio.2021.01.012
84. Bittner SM, Smith BT, Diaz-Gomez L et al (2019) Fabrication and mechanical characterization of 3D printed vertical uniform and gradient scaffolds for bone and osteochondral tissue engineering. Acta Biomater 90:37–48. https://doi.org/10.1016/j.actbio.2019.03.041
85. Cao Y, Cheng P, Sang S et al (2021) Mesenchymal stem cells loaded on 3D-printed gradient poly(ε-caprolactone)/methacrylated alginate composite scaffolds for cartilage tissue engineering. Regen Biomater 8(3):rbab019. https://doi.org/10.1093/rb/rbab019
86. Radhakrishnan J, Manigandan A, Chinnaswamy P et al (2018) Gradient nano-engineered in situ forming composite hydrogel for osteochondral regeneration. Biomaterials 162:82–98. https://doi.org/10.1016/j.biomaterials.2018.01.056
87. Gao J, Ding X, Yu X et al (2021) Cell-free bilayered porous scaffolds for osteochondral regeneration fabricated by continuous 3D-printing using nascent physical hydrogel as ink. Adv Healthc Mater 10(3):2001404. https://doi.org/10.1002/adhm.202001404
88. Sobral JM, Caridade SG, Sousa RA et al (2011) Three-dimensional plotted scaffolds with controlled pore size gradients: effect of scaffold geometry on mechanical performance and cell seeding efficiency. Acta Biomater 7(3):1009–1018. https://doi.org/10.1016/j.actbio.2010.11.003
89. Diloksumpan P, Bolanos RV, Cokelaere S et al (2020) Orthotopic bone regeneration within 3D printed bioceramic scaffolds with region-dependent porosity gradients in an equine model. Adv Healthc Mater 9(10):e1901807. https://doi.org/10.1002/adhm.201901807
90. Melchels FPW, Tonnarelli B, Olivares AL et al (2011) The influence of the scaffold design on the distribution of adhering cells after perfusion cell seeding. Biomaterials 32(11):2878–2884. https://doi.org/10.1016/j.biomaterials.2011.01.023
91. Nune KC, Kumar A, Misra RDK et al (2017) Functional response of osteoblasts in functionally gradient titanium alloy mesh arrays processed by 3D additive manufacturing. Colloids Surf B Biointerf 150:78–88. https://doi.org/10.1016/j.colsurfb.2016.09.050
92. Zonderland J, Moroni L (2021) Steering cell behavior through mechanobiology in 3D: a regenerative medicine perspective. Biomaterials 268:120572. https://doi.org/10.1016/j.biomaterials.2020.120572
93. Diez-Escudero A, Harlin H, Isaksson P et al (2020) Porous polylactic acid scaffolds for bone regeneration: a study of additively manufactured triply periodic minimal surfaces and their osteogenic potential. J Tissue Eng 11:1–14. https://doi.org/10.1177/2041731420956541
94. Perez RA, Mestres G (2016) Role of pore size and morphology in musculo-skeletal tissue regeneration. Mater Sci Eng C Mater Biol Appl 61:922–939. https://doi.org/10.1016/j.msec.2015.12.087
95. Le Guehennec L, Van Hede D, Plougonven E et al (2020) In vitro and in vivo biocompatibility of calcium-phosphate scaffolds three-dimensional printed by stereolithography for bone regeneration. J Biomed Mater Res A 108(3):412–425. https://doi.org/10.1002/jbm.a.36823
96. Liu Z, Wu S, Li J et al (2021) Three-dimensional printed hydroxyapatite bone tissue engineering scaffold with antibacterial and osteogenic ability. J Biol Eng 15(1):21. https://doi.org/10.1186/s13036-021-00273-6
97. Yadav LR, Chandran SV, Lavanya K et al (2021) Chitosan-based 3D-printed scaffolds for bone tissue engineering. Int J Biol Macromol 183:1925–1938. https://doi.org/10.1016/j.ijbiomac.2021.05.215
98. Casarrubios L, Gomez-Cerezo N, Sanchez-Salcedo S et al (2020) Silicon substituted hydroxyapatite/VEGF scaffolds stimulate bone regeneration in osteoporotic sheep. Acta Biomater 101:544–553. https://doi.org/10.1016/j.actbio.2019.10.033
99. Habibovic P, Yuan H, van der Valk CM et al (2005) 3D microenvironment as essential element for osteoinduction by biomaterials. Biomaterials 26(17):3565–3575. https://doi.org/10.1016/j.biomaterials.2004.09.056
100. Kolesky DB, Homan KA, Skylar-Scott MA et al (2016) Three-dimensional bioprinting of thick vascularized tissues. Proc Natl Acad Sci USA 113(12):3179–3184. https://doi.org/10.1073/pnas.1521342113
101. Freeman FE, Pitacco P, Van Dommelen LHA et al (2020) 3D bioprinting spatiotemporally defined patterns of growth factors to tightly control tissue regeneration. Sci Adv 6(33):e5093. https://doi.org/10.1126/sciadv.abb5093
102. Kolesky DB, Truby RL, Gladman AS et al (2014) 3D bioprinting of vascularized, heterogeneous cell-laden tissue constructs. Adv Mater 26(19):3124–3130. https://doi.org/10.1002/adma.201305506
103. Lee VK, Kim DY, Ngo H et al (2014) Creating perfused functional vascular channels using 3D bio-printing technology. Biomaterials 35(28):8092–8102. https://doi.org/10.1016/j.biomaterials.2014.05.083
104. Mori N, Akagi Y, Imai Y et al (2020) Fabrication of perfusable vascular channels and capillaries in 3D liver-like tissue. Sci Rep 10(1):5646. https://doi.org/10.1038/s41598-020-62286-3
105. Sekine H, Shimizu T, Sakaguchi K et al (2013) In vitro fabrication of functional three-dimensional tissues with perfusable blood vessels. Nat Commun 4:1399. https://doi.org/10.1038/ncomms2406
106. Wang Z, Wang H, Xiong J et al (2021) Fabrication and in vitro evaluation of PCL/gelatin hierarchical scaffolds based on melt electrospinning writing and solution electrospinning for bone regeneration. Mater Sci Eng C Mater Biol Appl 128:112287. https://doi.org/10.1016/j.msec.2021.112287

107. Liu X, Chen M, Luo J et al (2021) Immunopolarization-regulated 3D printed-electrospun fibrous scaffolds for bone regeneration. Biomaterials 276:121037. https://doi.org/10.1016/j.biomaterials.2021.121037
108. Wan S, Fu X, Ji Y et al (2018) FAK- and YAP/TAZ dependent mechanotransduction pathways are required for enhanced immunomodulatory properties of adipose-derived mesenchymal stem cells induced by aligned fibrous scaffolds. Biomaterials 171:107–117. https://doi.org/10.1016/j.biomaterials.2018.04.035
109. Spiller KL, Anfang RR, Spiller KJ et al (2014) The role of macrophage phenotype in vascularization of tissue engineering scaffolds. Biomaterials 35(15):4477–4488. https://doi.org/10.1016/j.biomaterials.2014.02.012
110. Sridharan R, Cameron AR, Kelly DJ et al (2015) Biomaterial based modulation of macrophage polarization: a review and suggested design principles. Mater Today 18(6):313–325. https://doi.org/10.1016/j.mattod.2015.01.019
111. Su N, Gao PL, Wang K et al (2017) Fibrous scaffolds potentiate the paracrine function of mesenchymal stem cells: a new dimension in cell-material interaction. Biomaterials 141:74–85. https://doi.org/10.1016/j.biomaterials.2017.06.028
112. Wang S, Hashemi S, Stratton S et al (2021) The effect of physical cues of biomaterial scaffolds on stem cell behavior. Adv Healthc Mater 10(3):2001244. https://doi.org/10.1002/adhm.202001244
113. Raja N, Yun HS (2016) A simultaneous 3D printing process for the fabrication of bioceramic and cell-laden hydrogel core/shell scaffolds with potential application in bone tissue regeneration. J Mater Chem B 4(27):4707–4716. https://doi.org/10.1039/c6tb00849f
114. Miller JS, Stevens KR, Yang MT et al (2012) Rapid casting of patterned vascular networks for perfusable engineered three-dimensional tissues. Nat Mater 11(9):768–774. https://doi.org/10.1038/nmat3357
115. Noor N, Shapira A, Edri R et al (2019) 3D printing of personalized thick and perfusable cardiac patches and hearts. Adv Sci 6(11):1900344. https://doi.org/10.1002/advs.201900344
116. Ouyang L, Armstrong JPK, Chen Q et al (2020) Void-free 3D bioprinting for in-situ endothelialization and microfluidic perfusion. Adv Funct Mater 30(1):1908349. https://doi.org/10.1002/adfm.201908349
117. Luo C, Xie R, Zhang J et al (2020) Low-temperature three-dimensional printing of tissue cartilage engineered with gelatin methacrylamide. Tissue Eng Part C Methods 26(6):306–316. https://doi.org/10.1089/ten.TEC.2020.0053
118. Shao L, Gao Q, Xie C et al (2020) Directly coaxial 3D bioprinting of large-scale vascularized tissue constructs. Biofabrication 12(3):035014. https://doi.org/10.1088/1758-5090/ab7e76
119. Zhang YS, Arneri A, Bersini S et al (2016) Bioprinting 3D microfibrous scaffolds for engineering endothelialized myocardium and heart-on-a-chip. Biomaterials 110:45–59. https://doi.org/10.1016/j.biomaterials.2016.09.003
120. Li T, Zhai D, Ma B et al (2019) 3D printing of hot dog-like biomaterials with hierarchical architecture and distinct bioactivity. Adv Sci 6(19):1901146. https://doi.org/10.1002/advs.201901146
121. Wang C, Lai J, Li K et al (2021) Cryogenic 3D printing of dual-delivery scaffolds for improved bone regeneration with enhanced vascularization. Bioact Mater 6(1):137–145. https://doi.org/10.1016/j.bioactmat.2020.07.007
122. Ahlfeld T, Schuster FP, Forster Y et al (2019) 3D plotted biphasic bone scaffolds for growth factor delivery: biological characterization in vitro and in vivo. Adv Healthc Mater 8(7):e1801512. https://doi.org/10.1002/adhm.201801512
123. Ahlfeld T, Akkineni AR, Forster Y et al (2017) Design and fabrication of complex scaffolds for bone defect healing: combined 3D plotting of a calcium phosphate cement and a growth factor-loaded hydrogel. Ann Biomed Eng 45(1):224–236. https://doi.org/10.1007/s10439-016-1685-4
124. Liu CG, Zeng YT, Kankala RK et al (2018) Characterization and preliminary biological evaluation of 3D-printed porous scaffolds for engineering bone tissues. Materials 11(10):1832. https://doi.org/10.3390/ma11101832
125. Han X, Sun M, Chen B et al (2021) Lotus seedpod-inspired internal vascularized 3D printed scaffold for bone tissue repair. Bioact Mater 6(6):1639–1652. https://doi.org/10.1016/j.bioactmat.2020.11.019
126. Yuan H, Fernandes H, Habibovic P et al (2010) Osteoinductive ceramics as a synthetic alternative to autologous bone grafting. Proc Natl Acad Sci USA 107(31):13614–13619. https://doi.org/10.1073/pnas.1003600107
127. Piard C, Jeyaram A, Liu Y et al (2019) 3D printed HUVECs/MSCs cocultures impact cellular interactions and angiogenesis depending on cell-cell distance. Biomaterials 222:119423. https://doi.org/10.1016/j.biomaterials.2019.119423
128. Au P, Tam J, Fukumura D et al (2008) Bone marrow–derived mesenchymal stem cells facilitate engineering of long-lasting functional vasculature. Blood 111(9):4551–4558. https://doi.org/10.1182/blood-2007-10-118273
129. Unger RE, Sartoris A, Peters K et al (2007) Tissue-like self-assembly in cocultures of endothelial cells and osteoblasts and the formation of microcapillary-like structures on three-dimensional porous biomaterials. Biomaterials 28(27):3965–3976. https://doi.org/10.1016/j.biomaterials.2007.05.032
130. Vidal L, Kampleitner C, Krissian S et al (2020) Regeneration of segmental defects in metatarsus of sheep with vascularized and customized 3D-printed calcium phosphate scaffolds. Sci Rep 10(1):7068. https://doi.org/10.1038/s41598-020-63742-w
131. Entezari A, Roohani I, Li G et al (2019) Architectural design of 3D printed scaffolds controls the volume and functionality of newly formed bone. Adv Healthc Mater 8(1):e1801353. https://doi.org/10.1002/adhm.201801353
132. Reznikov N, Boughton OR, Ghouse S et al (2019) Individual response variations in scaffold-guided bone regeneration are determined by independent strain- and injury-induced mechanisms. Biomaterials 194:183–194. https://doi.org/10.1016/j.biomaterials.2018.11.026
133. Oladapo BI, Ismail SO, Bowoto OK et al (2020) Lattice design and 3D-printing of peek with $Ca_{10}(OH)(PO_4)_3$ and in-vitro bio-composite for bone implant. Int J Biol Macromol 165(Pt A):50–62. https://doi.org/10.1016/j.ijbiomac.2020.09.175
134. Ahmadi SM, Campoli G, Amin Yavari S et al (2014) Mechanical behavior of regular open-cell porous biomaterials made of diamond lattice unit cells. J Mech Behav Biomed Mater 34:106–115. https://doi.org/10.1016/j.jmbbm.2014.02.003
135. Luo Y, Zhai D, Huan Z et al (2015) Three-dimensional printing of hollow-struts-packed bioceramic scaffolds for bone regeneration. ACS Appl Mater Interf 7(43):24377–24383. https://doi.org/10.1021/acsami.5b08911
136. Zhang W, Feng C, Yang G et al (2017) 3D-printed scaffolds with synergistic effect of hollow-pipe structure and bioactive ions for vascularized bone regeneration. Biomaterials 135:85–95. https://doi.org/10.1016/j.biomaterials.2017.05.005
137. Feng C, Ma B, Xu M et al (2021) Three-dimensional printing of scaffolds with synergistic effects of micro-nano surfaces and hollow channels for bone regeneration. ACS Biomater Sci Eng 7(3):872–880. https://doi.org/10.1021/acsbiomaterials.9b01824
138. Kon E, Salamanna F, Filardo G et al (2021) Bone regeneration in load-bearing segmental defects, guided by biomorphic, hierarchically structured apatitic scaffold. Front Bioeng Biotechnol 9:734486. https://doi.org/10.3389/fbioe.2021.734486
139. Filardo G, Roffi A, Fey T et al (2020) Vegetable hierarchical structures as template for bone regeneration: new bio-ceramization

process for the development of a bone scaffold applied to an experimental sheep model. J Biomed Mater Res B Appl Biomater 108(3):600–611. https://doi.org/10.1002/jbm.b.34414
140. Filardo G, Kon E, Tampieri A et al (2014) New bio-ceramization processes applied to vegetable hierarchical structures for bone regeneration: an experimental model in sheep. Tissue Eng Part A 20(3–4):763–773. https://doi.org/10.1089/ten.TEA.2013.0108
141. Feng C, Zhang W, Deng C et al (2017) 3D printing of lotus root-like biomimetic materials for cell delivery and tissue regeneration. Adv Sci 4(12):1700401. https://doi.org/10.1002/advs.201700401
142. Gu J, Zhang Q, Geng M et al (2021) Construction of nanofibrous scaffolds with interconnected perfusable microchannel networks for engineering of vascularized bone tissue. Bioact Mater 6(10):3254–3268. https://doi.org/10.1016/j.bioactmat.2021.02.033
143. Konka J, Buxadera-Palomero J, Espanol M et al (2021) 3D printing of hierarchical porous biomimetic hydroxyapatite scaffolds: adding concavities to the convex filaments. Acta Biomater 134:744–759. https://doi.org/10.1016/j.actbio.2021.07.071
144. Won JE, Lee YS, Park JH et al (2020) Hierarchical microchanneled scaffolds modulate multiple tissue-regenerative processes of immune-responses, angiogenesis, and stem cell homing. Biomaterials 227:119548. https://doi.org/10.1016/j.biomaterials.2019.119548
145. Lian M, Sun B, Han Y et al (2021) A low-temperature-printed hierarchical porous sponge-like scaffold that promotes cell-material interaction and modulates paracrine activity of MSCs for vascularized bone regeneration. Biomaterials 274:120841. https://doi.org/10.1016/j.biomaterials.2021.120841
146. Li T, Ma H, Ma H et al (2019) Mussel-inspired nanostructures potentiate the immunomodulatory properties and angiogenesis of mesenchymal stem cells. ACS Appl Mater Interf 11(19):17134–17146. https://doi.org/10.1021/acsami.8b22017
147. Liu Y, Yang S, Cao L et al (2020) Facilitated vascularization and enhanced bone regeneration by manipulation hierarchical pore structure of scaffolds. Mater Sci Eng C Mater Biol Appl 110:110622. https://doi.org/10.1016/j.msec.2019.110622
148. Geng M, Zhang Q, Gu J et al (2021) Construction of a nanofiber network within 3D printed scaffolds for vascularized bone regeneration. Biomater Sci 9(7):2631–2646. https://doi.org/10.1039/d0bm02058c
149. Reed S, Lau G, Delattre B et al (2016) Macro- and micro-designed chitosan-alginate scaffold architecture by three-dimensional printing and directional freezing. Biofabrication 8(1):015003. https://doi.org/10.1088/1758-5090/8/1/015003
150. Hong MH, Kim YH, Ganbat D et al (2014) Capillary action: enrichment of retention and habitation of cells via microchanneled scaffolds for massive bone defect regeneration. J Mater Sci Mater Med 25(8):1991–2001. https://doi.org/10.1007/s10856-014-5225-1
151. Polak SJ, Rustom LE, Genin GM et al (2013) A mechanism for effective cell-seeding in rigid, microporous substrates. Acta Biomater 9(8):7977–7986. https://doi.org/10.1016/j.actbio.2013.04.040
152. Lim KS, Baptista M, Moon S et al (2019) Microchannels in development, survival, and vascularisation of tissue analogues for regenerative medicine. Trends Biotechnol 37(11):1189–1201. https://doi.org/10.1016/j.tibtech.2019.04.004
153. Sprio S, Ruffini A, Tampieri A (2021) Biomorphic transformations: a leap forward in getting nanostructured 3-D bioceramics. Front Chem 9:728907. https://doi.org/10.3389/fchem.2021.728907
154. Du D, Asaoka T, Ushida T et al (2014) Fabrication and perfusion culture of anatomically shaped artificial bone using stereolithography. Biofabrication 6(4):045002. https://doi.org/10.1088/1758-5082/6/4/045002
155. Ding C, Qiao Z, Jiang W et al (2013) Regeneration of a goat femoral head using a tissue-specific, biphasic scaffold fabricated with CAD/CAM technology. Biomaterials 34(28):6706–6716. https://doi.org/10.1016/j.biomaterials.2013.05.038
156. Ren PG, Irani A, Huang Z et al (2011) Continuous infusion of UHMWPE particles induces increased bone macrophages and osteolysis. Clin Orthop Relat Res 469(1):113–122. https://doi.org/10.1007/s11999-010-1645-5
157. Lewallen EA, Riester SM, Bonin CA et al (2015) Biological strategies for improved osseointegration and osteoinduction of porous metal orthopedic implants. Tissue Eng Part B Rev 21(2):218–230. https://doi.org/10.1089/ten.TEB.2014.0333
158. Lee KG, Lee KS, Kang YJ et al (2018) Rabbit calvarial defect model for customized 3D-printed bone grafts. Tissue Eng Part C Methods 24(5):255–262. https://doi.org/10.1089/ten.TEC.2017.0474
159. Ku JK, Lee KG, Ghim MS et al (2021) Onlay-graft of 3D printed Kagome-structure PCL scaffold incorporated with rhBMP-2 based on hyaluronic acid hydrogel. Biomed Mater 16(5):055004. https://doi.org/10.1088/1748-605X/ac0f47
160. Bao X, Zhu L, Huang X et al (2017) 3D biomimetic artificial bone scaffolds with dual-cytokines spatiotemporal delivery for large weight-bearing bone defect repair. Sci Rep 7(1):7814. https://doi.org/10.1038/s41598-017-08412-0
161. Alluri R, Song X, Bougioukli S et al (2019) Regional gene therapy with 3D printed scaffolds to heal critical sized bone defects in a rat model. J Biomed Mater Res A 107(10):2174–2182. https://doi.org/10.1002/jbm.a.36727
162. Khalyfa A, Vogt S, Weisser J et al (2007) Development of a new calcium phosphate powder-binder system for the 3D printing of patient specific implants. J Mater Sci Mater Med 18(5):909–916. https://doi.org/10.1007/s10856-006-0073-2
163. Lee JS, Park TH, Ryu JY et al (2021) Osteogenesis of 3D-printed PCL/TCP/bdECM scaffold using adipose-derived stem cells aggregates; an experimental study in the canine mandible. Int J Mol Sci 22(11):5409. https://doi.org/10.3390/ijms22115409
164. Dewey MJ, Nosatov AV, Subedi K et al (2021) Inclusion of a 3D-printed hyperelastic bone mesh improves mechanical and osteogenic performance of a mineralized collagen scaffold. Acta Biomater 121:224–236. https://doi.org/10.1016/j.actbio.2020.11.028
165. Holmes B, Bulusu K, Plesniak M et al (2016) A synergistic approach to the design, fabrication and evaluation of 3D printed micro and nano featured scaffolds for vascularized bone tissue repair. Nanotechnology 27(6):064001. https://doi.org/10.1088/0957-4484/27/6/064001
166. Robles-Linares JA, Ramirez-Cedillo E, Siller HR et al (2019) Parametric modeling of biomimetic cortical bone microstructure for additive manufacturing. Materials 12(6):913. https://doi.org/10.3390/ma12060913
167. Le BQ, Nurcombe V, Cool SM et al (2017) The components of bone and what they can teach us about regeneration. Materials 11(1):14. https://doi.org/10.3390/ma11010014
168. Predoi-Racila M, Crolet JM (2008) Human cortical bone: the SiNuPrOs model. Comput Methods Biomech Biomed Eng 11(2):169–187. https://doi.org/10.1080/10255840701695140
169. Cowin SC, Cardoso L (2015) Blood and interstitial flow in the hierarchical pore space architecture of bone tissue. J Biomech 48(5):842–854. https://doi.org/10.1016/j.jbiomech.2014.12.013
170. Conward M, Samuel J (2016) Machining characteristics of the haversian and plexiform components of bovine cortical bone. J Mech Behav Biomed Mater 60:525–534. https://doi.org/10.1016/j.jmbbm.2016.03.017
171. Mazzoni S, Mohammadi S, Tromba G et al (2017) Role of corticocancellous heterologous bone in human periodontal ligament stem cell xeno-free culture studied by synchrotron radiation phase-

contrast microtomography. Int J Mol Sci 18(2):364. https://doi.org/10.3390/ijms18020364
172. Li S, Song C, Yang S et al (2019) Supercritical CO_2 foamed composite scaffolds incorporating bioactive lipids promote vascularized bone regeneration via Hif-1α upregulation and enhanced type H vessel formation. Acta Biomater 94:253–267. https://doi.org/10.1016/j.actbio.2019.05.066
173. Shah FA, Omar O, Suska F et al (2016) Long-term osseointegration of 3D printed CoCr constructs with an interconnected open-pore architecture prepared by electron beam melting. Acta Biomater 36:296–309. https://doi.org/10.1016/j.actbio.2016.03.033
174. Shi J, Zhu L, Li L et al (2018) A TPMS-based method for modeling porous scaffolds for bionic bone tissue engineering. Sci Rep 8(1):7395. https://doi.org/10.1038/s41598-018-25750-9
175. Vanderburgh JP, Fernando SJ, Merkel AR et al (2017) Fabrication of trabecular bone-templated tissue-engineered constructs by 3D inkjet printing. Adv Healthc Mater 6(22):1700369. https://doi.org/10.1002/adhm.201700369
176. Zhang M, Lin R, Wang X et al (2020) 3D printing of Haversian bone-mimicking scaffolds for multicellular delivery in bone regeneration. Sci Adv 6(12):eaa6725. https://doi.org/10.1126/sciadv.aaz6725
177. Griffith LG, Swartz MA (2006) Capturing complex 3D tissue physiology in vitro. Nat Rev Mol Cell Biol 7(3):211–224. https://doi.org/10.1038/nrm1858
178. Zhang B, Zhang M, Sun Y et al (2021) Haversian bone-mimicking bioceramic scaffolds enhancing MSC-macrophage osteo-imunomodulation. Progr Nat Sci Mater Int 31(6):883–890. https://doi.org/10.1016/j.pnsc.2021.04.008
179. Murphy SV, Atala A (2014) 3D bioprinting of tissues and organs. Nat Biotechnol 32(8):773–785. https://doi.org/10.1038/nbt.2958
180. Ribeiro A, Blokzijl MM, Levato R et al (2017) Assessing bioink shape fidelity to aid material development in 3D bioprinting. Biofabrication 10(1):014102. https://doi.org/10.1088/1758-5090/aa90e2
181. Ouyang L, Highley CB, Rodell CB et al (2016) 3D printing of shear-thinning hyaluronic acid hydrogels with secondary cross-linking. ACS Biomater Sci Eng 2(10):1743–1751. https://doi.org/10.1021/acsbiomaterials.6b00158
182. Daly AC, Pitacco P, Nulty J et al (2018) 3D printed microchannel networks to direct vascularisation during endochondral bone repair. Biomaterials 162:34–46. https://doi.org/10.1016/j.biomaterials.2018.01.057
183. Twohig C, Helsinga M, Mansoorifar A et al (2021) A dual-ink 3D printing strategy to engineer pre-vascularized bone scaffolds in-vitro. Mater Sci Eng C Mater Biol Appl 123:111976. https://doi.org/10.1016/j.msec.2021.111976
184. Wei S, Ma JX, Xu L et al (2020) Biodegradable materials for bone defect repair. Mil Med Res 7(1):54. https://doi.org/10.1186/s40779-020-00280-6
185. Piard C, Baker H, Kamalitdinov T et al (2019) Bioprinted osteon-like scaffolds enhance in vivo neovascularization. Biofabrication 11(2):025013. https://doi.org/10.1088/1758-5090/ab078a
186. Zuo Y, Liu X, Wei D et al (2015) Photo-cross-linkable methacrylated gelatin and hydroxyapatite hybrid hydrogel for modularly engineering biomimetic osteon. ACS Appl Mater Interf 7(19):10386–10394. https://doi.org/10.1021/acsami.5b01433

Springer Nature or its licensor holds exclusive rights to this article under a publishing agreement with the author(s) or other rightsholder(s); author self-archiving of the accepted manuscript version of this article is solely governed by the terms of such publishing agreement and applicable law.